3-26-2002

Design Study of Triggered Isomer Heat Exchanger-Combustion Hybrid Jet Engine for High Altitude Flight

Christopher E. Hamilton

DESIGN STUDY OF TRIGGERED ISOMER HEAT EXCHANGER-COMBUSTION HYBRID JET ENGINE FOR HIGH ALTITUDE FLIGHT

THESIS

Christopher E. Hamilton, Captain, USAF

AFIT/GAE/ENY/02-6

DEPARTMENT OF THE AIR FORCE

AIR UNIVERSITY

AIR FORCE INSTITUTE OF TECHNOLOGY

Wright-Patterson Air Force Base, Ohio

Report Documentation Page

Report Date	Report Type	Dates Covered (from... to)
26 Mar 02	Final	Jun 2001 - Mar 2002

Title and Subtitle Design Study of Triggered Isomer Heat Exchanger-Combustion Hybrid Jet Engine for High Altitude Flight	**Contract Number**
	Grant Number
	Program Element Number
Author(s) Capt Christopher E. Hamilton, USAF	**Project Number**
	Task Number
	Work Unit Number
Performing Organization Name(s) and Address(es) Air Force Institute of Technology Graduate School of Engineering and Management (AFIT/EN) 2950 P Street WPAFB, OH 45433-7765	**Performing Organization Report Number** AFIT/GAE/ENY/02-6
Sponsoring/Monitoring Agency Name(s) and Address(es) AFRL/DEBE ATTN: P McDaniel Kirtland, NM	**Sponsor/Monitor's Acronym(s)**
	Sponsor/Monitor's Report Number(s)

Distribution/Availability Statement
Approved for public release, distribution unlimited

Supplementary Notes
The original document contains color images.

Abstract
This study investigated the possibility of utilizing a Triggered Isomer Heat Exchanger (TIHE) within a conventional jet engine in order to increase the endurance of a High Altitude Long Endurance (HALE) Intelligence, Surveillance, and Reconnaissance (ISR) aircraft. Optimizations of the conventional and TIHE engines along with selection of a switchover flight condition, where the aircraft switches from combustion to TIHE operations, were made utilizing engine design and mission analysis software. Radiation shield weights were determined utilizing point source gamma ray shielding methods. The jet engine best suited for the hybrid use, where both combustion and TIHE components located in a single engine, was a mixed stream turbofan engine flying both the conventional and TIHE legs of the mission, with a switchover Mach of 0.4 and switchover altitude of 40,000 ft. With the single hybrid engine, including shield weights and modifications, endurance could easily be extended into weeks instead of days, while also resulting in a 20% drop in takeoff weight of current vehicles. The reduction in weight was due mainly to lower fuel requirements.

Subject Terms Triggered Isomer, High Altitude Long Endurance, Intelligence, Surveillance, Reconnaissance, Aircraft Propulsion, Turbofan	
Report Classification unclassified	**Classification of this page** unclassified
Classification of Abstract unclassified	**Limitation of Abstract** UU
Number of Pages 111	

The views expressed in this thesis are those of the author and do not reflect the official policy or position of the United States Air Force, Department of Defense, or the U. S. Government.

AFIT/GAE/ENY/02-6

DESIGN STUDY OF TRIGGERED ISOMER HEAT EXCHANGER-COMBUSTION HYBRID JET ENGINE FOR HIGH ALTITUDE FLIGHT

THESIS

Presented to the Faculty

Department of Aeronautical and Astronautical Engineering

Graduate School of Engineering and Management

Air Force Institute of Technology

Air University

Air Education and Training Command

In Partial Fulfillment of the Requirements for the

Degree of Master of Science in Aeronautical Engineering

Christopher E. Hamilton, B.S.A.E.

Captain, USAF

March 2002

AFIT/GAE/ENY/02-6

DESIGN STUDY OF TRIGGERED ISOMER HEAT EXCHANGER-COMBUSTION HYBRID JET ENGINE FOR HIGH ALTITUDE FLIGHT

Christopher E. Hamilton, B.S.A.E.
Captain, USAF

Approved:

Paul I. King (Thesis Advisor)	13 Mar 02 date
Milton E. Franke (Thesis Advisor)	13 MAR 2002 date
William C. Elrod (Member)	13 Mar 2002 date
Ralph A. Anthenien Jr. (Member)	13 Mar 02 date

Acknowledgements

I would like to first like to thank Dr. King and Dr. Franke for their direction and motivation. Working with two advisors had its challenges, but in the end the two perspectives allowed me to look at the problem at hand from several angles and helped me produce a better product. The many question and answer sessions that we had helped me stay focused on the research goal. I learned a great deal from you gentlemen.

I had assistance in my research from many other sources but two gentlemen provided invaluable help. Surinder Dhaliwal from ASC/RAV aided me in finding information about HALE UAVs, when I seemed to be going in circles. Dr. Jack Mattingly, besides being the author of my main engine design references, came to the rescue when a programming glitch in the software I was using seemed cause a halt in my research. He went above and beyond in helping me with AEDsys and ONX during the holidays.

Of course, social support was essential to my ability to finish this research. My fellow Aero students provided camaraderie and important aid in the little details and in keeping perspective. My friends and family helped me see over the obstacles and keep focused, while also giving me an outlet when I needed it. Special thanks to Kate; I don't think I could have done so much in so little time without your support and care.

Christopher Hamilton

Table of Contents

Page

Page

Page

Table of Figures

Page

Page

List of Tables

Page

Nomenclature

Symbol	Description
α	Bypass ratio
β	Current Weight Fraction
Δ	Change in values from initial point to final point
μ	Linear attenuation coefficient (cm^{-1})
ρ	Density (lbm/ft^3)
Ψ	Intensity or energy fluence rate (W/m^2)
μ/ρ	Mass attenuation coefficient (cm^2/g)
η_b	Burner efficiency
π_C	Overall Compressor Pressure Ratio
π_C'	Fan Pressure ratio
μ_{en}/ρ	Mass energy absorption coefficient (m^2/kg)
ε_{heat}	Heat conversion efficiency
Π_i	Weight fraction
τ_T	Turbine temperature ratio
μx	Relaxation length
σ_Y	Yield Stress (psi)
A	Cross-sectional Area (ft^2) or (m^2)
A_0^*	Choked freestream area (ft^2)
A_1	Inlet Area (ft^2)
A_{10}	Engine exit area (ft^2)
A_9	Nozzle exit area (ft^2)
ANP	Aircraft Nuclear Propulsion program
AR	Aspect Ratio
B	Dose buildup factor
C_D	Coefficient of Drag
C_{Dmin}	Value of C_D at C_{Lmin}
CE	Radiation output at source (W)
C_L	Coefficient of Lift
C_{Lmin}	Minimum value of C_L
D	Drag (lbf)
d	Thickness of hoop (in)

e_{stored}	Mass specific energy stored (W/kg)
eV	Electron Volt
F	Uninstalled Thrust (lbf)
F/m_0	Uninstalled specific Thrust
g_0	Acceleration of gravity (ft/sec^2)
g_c	Newton's gravitational constant (32.174 lbm*ft/(lbf*sec^2))
h	Altitude (ft)
HALE	High Altitude Long Endurance
Hf	Hafnium
h_{pr}	Heating value of fuel (BTU/lbm)
I	Intensity at target (rad/sec)
I_0	Intensity at target unshielded (rad/sec)
ISR	Intelligence, Surveillance, and Reconnaissance
K'	Inviscid induced Drag
K"	Viscous skin friction and pressure drag
L	Lift (lbf)
l	Nozzle length (ft)
lbf	Pounds force
lbm	Pounds mass
LPC π	Low pressure compressor pressure ratio
Lu	Lutetium
M	Mach number
m_0	Mass flow rate at station 0 (lbm/sec)
M_0	Freestream Mach Number
m_{fdot}	Fuel consumption rate (lbm/sec)
n	Load factor
NEPA	Nuclear Energy for the Propulsion of Aircraft Program
nmi	Nautical mile
P_{max}	Maximum Internal Pressure (psi)
P_s	Weight specific excess power
P_{t3}	Compressor Exit Stagnation Pressure (psi)
Q_{burner}	Heat power required by TIHE (BTU/sec) or (W)
r	Radius (in, ft, or m) or distance from source (m)
R	Additional Drag due to stores or landing gear
S	Wing Surface Area (ft^2) or Uninstalled thrust specific fuel consumption

T	Installed Thrust (lbf)
t	Time (sec)
Ta	Tantalum
tfm	Mixed stream turbofan
tfs	Split stream turbofan
TI	Triggered Isomer
TIHE	Triggered Isomer Heat Exchanger
tj	Dual spool turbojet
tjs	Single spool turbojet
tp	Turboprop
TSFC	Installed Thrust Specific Fuel Consumption
T_{T3}	Compressor Exit Temperature (°R)
T_{T4}	Turbine Inlet Temperature (°R)
UAV	Unmanned Aerial Vehicle
V	Velocity (ft/sec)
W	Weight (lbf)
W_{final}	Final leg weight (lbf)
$W_{initial}$	Initial leg weight (lbf)
W_{TO}	Take off Weight (lbf)
x	Shield thickness (cm)

ABSTRACT

This study investigated the possibility of utilizing a Triggered Isomer Heat Exchanger (TIHE) within a conventional jet engine in order to increase the endurance of a High Altitude Long Endurance (HALE) Intelligence, Surveillance, and Reconnaissance (ISR) aircraft. Optimizations of the conventional and TIHE engines along with selection of a switchover flight condition, where the aircraft switches from combustion to TIHE operations, were made utilizing engine design and mission analysis software. Radiation shield weights were determined utilizing point source gamma ray shielding methods. The jet engine best suited for the hybrid use, where both combustion and TIHE components located in a single engine, was a mixed stream turbofan engine flying both the conventional and TIHE legs of the mission, with a switchover Mach of 0.4 and switchover altitude of 40,000 ft. With the single hybrid engine, including shield weights and modifications, endurance could easily be extended into weeks instead of days, while also resulting in a 20% drop in takeoff weight of current vehicles. The reduction in weight was due mainly to lower fuel requirements.

DESIGN STUDY OF TRIGGERED ISOMER HEAT EXCHANGER-COMBUSTION HYBRID JET ENGINE FOR HIGH ALTITUDE FLIGHT

1. Introduction

1.1 Motivation

With the advent of nuclear fission in the 1940's and the rapid development of aerospace propulsion systems during that same time, it seemed that the idea of powering the engines of aircraft and spacecraft with nuclear energy was an ideal merger of these two research thrusts. Preliminary work was done on developing nuclear powered rockets, jet engines, and ramjet engines during the late 1940s and throughout the 1950s (1, 2, 3). Both the US and USSR conducted rigorous research and development programs in this field, but ultimately cancelled their respective programs, due to technical difficulties and growing safety concerns.

For the past 40 years, little research has been done specifically relating to nuclear powered jet engines. Recent discoveries, in the field of controlled or triggered nuclear decay (4, 5), along with 40 years in the advancement of materials, airframe design, and jet engine development, have reinvigorated the possibility of running aircraft on nuclear power. Nuclear power could conceivably provide aircraft with compact heat sources allowing larger thrust levels than conventional chemical combustion systems can provide, as well as practically eliminating endurance limitations based on fuel requirements (2).

If this new power source can be utilized to provide heat energy to jet engines, it could dramatically change flight envelopes, costs, and capabilities of aerospace vehicles. High drag losses, which occur during low altitude flight, could be compensated by these propulsion systems; changing the fundamental way flight paths are developed. Flight times could be reduced by hours, if the need for refueling was eliminated. Thrust to weight values of these engines could allow for vertical or short runway takeoffs to become commonplace, imaginably eliminating the need for large runways.

While this idea has tremendous potential, research must begin in an orderly and progressive way. Basic systems need to be designed and suitable first-step applications need to be developed. Research into replacing a combustion section of a turbojet engine, with a triggered isomer heat exchanger represented the start of this process, by showing that the concept was feasible (6).

1.2 Problem Statement

The goal of this study was to develop methods for selecting jet engine configuration and flight path adjustments as well as estimating component weights for a two-stage High Altitude Long Endurance Unmanned Aerial Vehicle. The two stages being a conventional chemical combustion heat source powered flight segment and a triggered isomer heat exchanger powered segment. It was planned to utilize the Global Hawk UAV as a baseline representative of a generic HALE-UAV, in order to compare performance of the new two-stage approach with the current performance.

The approach selected for this study used traditional engine design and mission analysis methods to determine the fuel consumption of the traditional portion of the mission and the power requirements for the Triggered isomer heat exchanger (TIHE) portion of the mission for different engine types. The use of a range of switchover flight conditions allowed for the optimization of not only the engine type but also the flight path, to an extent. Once an optimized engine and flight path were selected, shield weights were calculated using point source gamma radiation shielding methods.

With all of this information, a direct weight comparison of the current and proposed vehicles could be made. The final results, while important, were of equal value to the methods developed to get the results. This study represents a first step at determining application-based requirements for this new Triggered Isomer Research Program.

1.3 Thesis Overview and General Comments

This work is organized into five chapters along with three appendices. Chapter 2 contains information about the history of and results from research conducted on nuclear powered aircraft, as well as background information on the triggered isomer research program. Chapter 3 represents a discussion of methods developed and used for this research, along with explanation of pertinent theories. This chapter also explains the two programs used during this research. Chapter 4 presents the results of this study, including conventional and TIHE engine selections along with component weight calculations. Chapter 5 provides closure, in the way of overall conclusions of the research and

recommendations for future study. Several appendices have been included that summarize results discussed in Chapter 4.

A short discussion about the unit systems used in this document is necessary. Due to the common practice, in engine and aircraft design of using English engineering units, the values used in these calculations are displayed primarily as English units. SI units are preferred, in general, for most other engineering applications and have been included in parentheses. Radiation calculations are made in SI units as is common in that field, however shield weights have been converted into English units for consistency within this report. In some cases, graphs presented will mix units.

2. Background/History

Before a study of this type could be started, information on several pertinent topics needed to be gathered and examined. Since the current research was going to involve Triggered Isomer (TI) physics, High Altitude Long Endurance (HALE) aircraft, Unmanned Aerial Vehicles (UAVs), and heat exchanger-powered jet engines; previous work in these areas were studied.

2.1 Triggered Isomer Program

The first area to be examined is triggered isomer physics research. While research in radioisotope decay is not new, the ability to trigger a large release of this energy on demand is a recent discovery. The Directed Energy Directorate of the Air Force Research Laboratory has been working in this field for the past several years and a joint Department of Defense and Department of Energy effort has been created to pursue this technology (5).

In 1998, University of Texas researchers led by Dr. Carl Collins were able to trigger significantly increased energy decay in a Hafnium isomer sample using a dental X-ray unit (4). The decay of the Hafnium in this case was a cascade of Gamma rays and X-rays of varying energy levels. Some of the X-rays in the cascade were similar in power and wavelength to the triggering X-rays from the dental device. If a means of reflecting the X-rays can be incorporated into a reactor, a chain reaction might be

possible. This would allow for a near instantaneous decay and the creation of a controllable power source. (5: 1)

This very compact power source could provide large amounts of heat. Aircraft and spacecraft could utilize this new power source, if it was made part of a high thrust-to-weight heat exchanger propulsion system. Rockets, or even jet engines, could be modified or redesigned to utilize this propulsion system in order to gain specific impulse or endurance values that are not possible with conventional combustion techniques.

An important factor that separates this triggered isomer reaction from fission reactions is that the radiation output is significantly less. Normal fission reactions, that have been proposed to drive rockets and jet engines, produce not only gamma radiation but also release neutrons and fission products, which would significantly increase shielding requirements, perhaps offsetting the weight reductions from the compact heat source. Gamma radiation, the only significant radiation product from TI reactions, while still dangerous, requires less shielding (5).

One of the studies commissioned by the triggered isomer program was a feasibility study of replacing outright a combustion section of an off-the-shelf turbojet engine with a solid-state heat exchanger (6). This study, utilizing current computational fluid dynamics and heat transfer methods, was able to show that a J-57 turbojet engine could provide equal thrust with a combustor or a heat exchanger at sea level static conditions. Several conclusions were made in this study.

The first was that if the heat generation rate could be controlled and that the heat exchanger material itself was made from the isomer, several different configurations could be utilized to be suitable replacements for the combustor. Issues of manufacturing

and development of the triggering and control system were left as areas for further research.

The second conclusion was that the ability of this heat exchanger to supply sufficient heating to the flow increases with higher altitudes. Due to the thermodynamics involved in engine performance at higher altitudes, heating requirements also drop off. This results in lower heat generation rates and reduced radiation output, thereby extending component lifetime.

The final conclusion was that this heating source would greatly increase aircraft endurance and "could drastically change the operating paradigms for many missions."(6: 5-2) Heat exchanger geometry could be optimized for specific aircraft and missions that would result in even more efficient turbojet engines.

2.2 High Altitude Long Endurance Mission study

The research done so far on TI reactor systems shows that it has the potential of being an enabling technology for aerospace propulsion (5). Possible applications for atmospheric flight include: highly maneuverable fighter/attack aircraft; long range cargo or passenger flight; long endurance intelligence, surveillance, and reconnaissance (ISR) platforms; long endurance communication relay platforms; and very long range cruise missiles. Rocket propulsion could also be enhanced resulting in significantly lower launch costs and shorter trip times to other planets.

As can be imagined the possible applications are numerous, so a particular mission needed to be selected, in order to do a more detailed study of design parameters.

All of these missions were considered in the current study, and several important aspects of research done to date, as well as probable priorities, were used to narrow the mission to a suitable candidate for study. Due to the research already conducted by Hartsfield (6), it was deemed that utilizing the TIHE system to power jet engines held promise. Rocket applications are still very much possible and should be studied. This decision to look only at jet engines narrowed the field down to aircraft.

Of the possible aircraft missions, the benefits of extended endurance impact heavily on the ISR platforms. Limiting the scope of this study to ISR aircraft, does not degrade the value of studying other missions, but allows for further depth into the design process. Many ISR aircraft fly at high altitudes to avoid surface threats and to allow larger area coverage. Slow flight allows for longer loiter times over the areas of interest. Both of these aspects of ISR platforms lower required thrust to maintain flight and make this mission ripe for TIHE application.

Due to radiation concerns, the first application of a TIHE powered jet engine will likely be on Unmanned Aerial Vehicles. In the case of HALE missions used in the ISR vehicles, this is advantageous since life support requirements become prohibitive very quickly due to mission duration and altitude.

With the selection of the HALE-UAV mission, it is important to note that such an aircraft has been recently produced and is flying operational missions. The Global Hawk aircraft, built by Northrop-Grumman for the United States Air Force, is the first High Altitude ISR UAV in production. The Global Hawk program started in 1994 as an Advanced Concept Technology Demonstrator and is currently completing its engineering, manufacturing and development phase (7). It has successfully been tested in

action as part of the Department of Defense's Operation Enduring Freedom over Afghanistan.

Since this aircraft represents the current leading edge of technology in the realm of HALE UAVs designed for ISR missions, it is an obvious choice for a baseline vehicle. Utilizing the current configuration of the Global Hawk will allow for comparison of weights and performance when utilizing the TIHE power source.

2.3 Global Hawk UAV

The Global Hawk UAV is an ISR platform that provides high altitude, long duration coverage. It has a 44.4 ft (13.53 m) long by 4.8 ft (1.46 m) wide fuselage with a wingspan of 116.2 ft (35.42 m), a wing area of 540 ft^2 (50.17 m^2) and an aspect ratio of 25. Takeoff weight is 25,600 lbf (113.87 kN), with a 1,900 lbf (8.45 kN) payload and 14,500 lbf (64.5 kN) of fuel. The vehicle is powered by a single Allison AE3007H high bypass, dual spool, axial-flow turbofan engine with 8,290 lbf (36.9 kN) of uninstalled sea level static thrust (7, 8, 9, 10).

The current range of the Global Hawk is a 1,200 nautical mile (nmi) (2,221 km) radius with 24 hours on station, with a planned extension to a 3,000 nmi (5,552 km) range radius. Its loiter altitude is between 50,000 (15.24 km) and 65,000 ft (19.8 km). Its nominal mission profile will be discussed in Chapter 3.

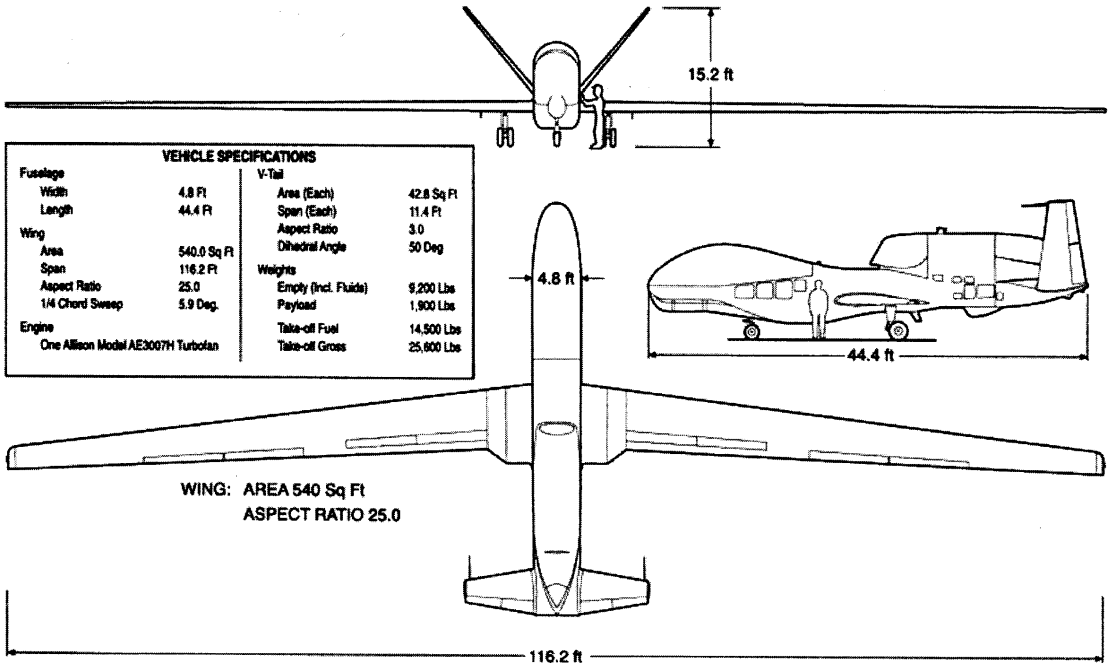

Figure 1: Global Hawk Air Vehicle Outline (9)

2.4 History of Nuclear Powered Aircraft Development

With the first success of a triggered isomer reaction occurring only recently, very little research has been completed in the design of propulsion systems utilizing this power source. Other than Hartsfield's research (6) on applications using a turbojet engine, the author found no published work in the field of TIHE powered aircraft. While the specific reaction is new, the concept of using nuclear power in aircraft was studied extensively by both the United States and the Soviet Union throughout the late 1940's, 1950's and early 1960's. Important concepts applicable to both fission and TI reactions were researched and are listed here.

2.4.1 NEPA to ANP. The United States began its fission powered aircraft research in 1946 by authorizing the Fairchild Engine and Airplane Corporation to conduct a feasibility study for using nuclear energy for the propulsion of aircraft (NEPA). Preliminary research was done at Oak Ridge National Laboratory where other nuclear research was being accomplished. In 1948, the Atomic Energy Commission created a separate study group at Massachusetts Institute of Technology (MIT) to study the feasibility of nuclear propulsion for aircraft. This study concluded in a report, called the "Lexington Report," that nuclear propulsion was feasible and that it could be achieved in 15 years with a price tag of over one billion dollars. (2, 11)

Due to the findings of the Lexington group, the two separate research efforts were combined in 1950, into a more focused program called the Aircraft Nuclear Propulsion (ANP) program. This program's goals were to develop information on reactor materials and shielding, as well as creating designs for aircraft and power plants within a 3-5 year time span. In 1951, demonstration of nuclear flight was added to the list of goals. Throughout the 1950s, funding and priorities issues caused significant slowdown of achieving the set goals. Development occurred but at a much slower pace than originally thought.

Several projects developed within the ANP program including the Project Rover nuclear rocket, the Project Pluto nuclear ramjet, and the Snap nuclear auxiliary power system programs (2). The manned aircraft program remained the major focus of the ANP and several important research projects were contracted out. These projects included airframe development, jet engine and reactor design, and radiation shielding.

2.4.2 ANP Airframe Development. Airframe development began with early estimates pointing to the feasibility of a supersonic manned bomber. Technical issues quickly interfered with the concept, which resulted in the decision to convert a B-36 into a flying subsonic nuclear propulsion test-bed instead. The contract for this work was awarded to the Convair Division of General Dynamics Corporation, where the modified B-36 would be redesignated the X-6 (12). This aircraft was later used as a test-bed for shield development after the X-6 program was cancelled. A second contract was awarded to Lockheed Aircraft Corporation to investigate the feasibility of a transonic nuclear bomber that would fly below 5,000 ft (1.5km). (12:70)

The Lockheed study pointed out important concepts that the aircraft designer utilizing a nuclear propulsion system must be aware of (13). The first being that since the reactors of the time were immense, on the order of tens of thousands of pounds, it represented a highly concentrated weight in the aircraft. In a conventional aircraft, the weight of the fuel is normally carried in the wings, spreading the total weight of the aircraft throughout the structure. This cannot be accomplished in an all-nuclear aircraft, where the reactor and majority of the shield weight is located near engines. This would require intensive structural consideration in the design.

The second concept was that powerful radiation emanating from the reactor must be attenuated to acceptable levels. This led to the concept of divided shielding, where the shield is divided into a section around the reactor and a section around the crew compartment. This reduced the total weight of shielding while providing necessary

radiation protection to the crew. The downside to divided shielding is that it allows for high radiation rates everywhere else in the airframe and into the environment.

Thirdly, since this propulsion system resulted in virtually unlimited flight endurance, several design challenges were introduced. The first is in calculating performance, where traditional methods take into account decreasing weight of the aircraft, due to fuel consumption. This lack of change in weight actually simplifies calculations, but the differences must be kept in mind during design work. Also, landing gears are normally designed to withhold the impact of about half the weight of the aircraft. This is not the case with the all-nuclear aircraft and therefore landing gear will have to be designed to withstand the full takeoff weight at landing.

2.4.3 Reactor and Engine Development. Development of the reactors and jet engines took two separate paths: a direct-cycle and an indirect-cycle system. Pratt & Whitney Aircraft Company was contracted, in 1953, to pursue the development of liquid-metal indirect cycle turbojet systems. The idea was to heat a liquid metal using the nuclear reactor and use the liquid metal to heat the air flow in a turbojet engine. Gains were made in reactor and heat exchanger designs, however the research never produced a test reactor (3).

The Direct-cycle program was run by General Electric and was extremely successful. In a direct cycle jet engine, the airflow in the engine is diverted after it leaves the compressor. It then enters the reactor, is heated directly, and then ducted back into the turbine section of the engine. In 1956, a ground test of a modified J-47 turbojet

engine was operated by a nuclear reactor in what was referred to as the Heat Transfer Reactor Experiment No. 1 (HTRE-1) (14).

This program was continued with more rigorous experiments, HTRE-2 and –3, that validated the concept of utilizing a nuclear reactor to power one or more turbojet engines. The final configuration for HTRE-3 powered two turbojet engines and was of the size to fit within an aircraft even though it was not designed to be a flight test model.

In addition to proving the basic concept, it also showed that a chemical-nuclear system could be used in tandem. All three engines were in reality hybrid combustion-nuclear turbojets. Each modified J-47 engine kept its combustion section and utilized it in starting the engine until the reactor could be brought up to the correct temperature. The chemical fuel was throttled down until the reactor provided all of the heat, at which point the fuel was shut off and the combustion process ceased. (14: 98) While the HTRE series was very successful, a flight test model was never built.

2.4.4 ANP Shield Development. Radiation shield research was done both on the ground with the runs of the HTRE tests, as well as on board the Convair B-36 that was cut from the X-6 program. The aircraft was fitted with a one-megawatt reactor weighing 36,000 lbf (160.1 kN), for shield research. The aircraft completed 47 successful flights during the remainder of the ANP program. Unfortunately, shielding requirements for the envisioned manned bomber were prohibitive. (12: 69-73)

With a nuclear test ban treaty being worked on by the nuclear-capable nations and the technical hurdles slowing down the 3-5 year plan proposed in 1950 to a crawl,

support for a nuclear powered aircraft dwindled. The ANP program was cancelled in 1961, despite the gains made. The technical hurdles that killed this nuclear fission powered program are important to any research dealing with nuclear powered flight.

Shielding weights were immense for the first aircraft design pursued. A low, fast, manned bomber was the goal throughout the NEPA/ANP program. This took advantage of the huge amounts of power available from fission reactions, but since radiation levels are directly related to the total power output of a reactor, radiation levels were also huge. Even after the decision was made to compromise the supersonic aircraft into a subsonic test vehicle, the goal was still a supersonic vehicle.

Materials, at the time, limited the heat that could be withstood by components of the engine. In addition, jet engines were relatively new and were inefficient compared to today's standards. Even with the difficulties, progress was being made. With time and effort, there is little doubt that a working test vehicle would have been constructed and flown.

3. Methods and Theory

This chapter covers the methods used to select mission parameters, engine type and parameters, and shield weight. Included in each method are important theoretical issues that need to be understood as part of the design and selection process.

3.1 Basic Flight Dynamics

In order to design engines for aircraft, consideration to the forces acting on the engine must be made. The basic forces acting on an aircraft can be summarized as Lift (L), Drag (D), Thrust (T), and Weight (W). Lift and drag are aerodynamic forces caused by a moving body interacting with the atmosphere. Weight is the force gravity exerts on the aircraft downward and thrust is the force applied to the aircraft from the engine(s).

A traditional equation for Lift is:

$$L = nW = \frac{1}{2} \rho V^2 C_L S \tag{1}$$

where

n = load factor

ρ = density (lbm/ft^3)

V = velocity (ft/sec)

C_L = lift coefficient

S = wing area (ft^2)

The amount of lift needed for an aircraft depends on whether the aircraft is flying straight and level, turning, climbing, or descending. Since all of these values are known at a specific moment in flight, the only independent variable becomes the lift coefficient. An equation used throughout the aircraft performance calculations rearranges eqn. (1) into a new form.

$$C_L = \frac{n\beta}{\frac{1}{2}\rho V^2}\left(\frac{W_{TO}}{S}\right) \tag{2}$$

where

W_{TO} = take-off weight

β = current weight fraction (W/W_{TO})

This grouping of terms assumes that the takeoff weight of the aircraft, the wing area, flight conditions, and the current weight of the aircraft are known. The value calculated for C_L usually determines the attitude of the wings with respect to the freestream air flow.

The equation for aerodynamic drag is similar to the lift equation:

$$D = \frac{1}{2}\rho V^2 C_D S \tag{3}$$

where C_D is the drag coefficient. C_D values are normally taken from wind tunnel testing, CFD, or flight test data and are based on C_L numbers. An equation for

calculating C_D, as a function of C_L, is called the Drag Polar and represents the sum of induced drag, skin friction, and pressure drag components.

$$C_D = K_1 C_L^2 + K_2 C_L + C_{D0} \tag{4}$$

$$K_1 = K' + K''$$

$$K_2 = -2 K'' C_{Lmin}^2$$

$$C_{D0} = C_{Dmin} + K'' C_{Lmin}^2$$

where

K' = inviscid induced drag
K'' = viscous skin friction and pressure drag
C_{Lmin} = minimum value of C_L
C_{Dmin} = value of C_D at C_{Lmin}

With a method to calculate lift and drag at each point in a mission, an easy means to determine thrust required is available. There are two different types of thrust maneuvers, one where thrust is equal to drag for steady flight or steady turns and the second is where the thrust is either larger or smaller than the drag leading the aircraft to accelerate or decelerate. The methods to determine required thrust will be explained in a later section.

3.2 High Altitude Long Endurance UAV Drag Polar

Drag Polar data can be roughly estimated for aircraft that fit into several categories (fighters, large passenger/cargo planes, small private planes) due to the

abundance of information available and the similarities within each type. For high aspect ratio (AR) HALE vehicles however, there is not a wealth of drag polar data available. Methods used for the other smaller AR vehicles break down in analysis of their high AR counterparts (15). Rough estimates were made based on existing HALE aircraft (16). This data was curve-fitted using the least squares method to match the drag calculations that would be used in the software. This information represents an estimate on drag for a similar aircraft and was deemed suitable for this study.

3.3 Mission Description

In engine design, three things must be determined before starting: aircraft configuration, mission description, and material tolerances. Since in this study, the Global Hawk aircraft is being used as a design reference, the aircraft configuration is, for the most part, predetermined. In this section we will examine the reference mission of the TIHE/conventional powered HALE UAV.

The notional Global Hawk mission calls for 8 main legs as illustrated in Fig. 2. The first is warm-up and takeoff and has a constraint that the aircraft must take off from a NATO standard runway of 8000 ft (2.44 km). This is followed by the climb-to-cruise leg that is planned to occur within a 200 nautical mile (nmi) (370 km) range. The Global Hawk then achieves a 3000 nmi (5,552 km) cruise climb to loiter target. The loiter phase of the mission has a minimum time on station (ToS) of 24 hours at an altitude of between 60-65,000 ft (18.3-19.8 km). At the end of the loiter phase, the aircraft initiates its egress cruise back 3000 nmi. This is followed by a descent to sea level scheduled for a 200 nmi

range. A one hour reserve loiter at sea level is the next leg. The aircraft completes its mission by landing at a NATO standard runway.

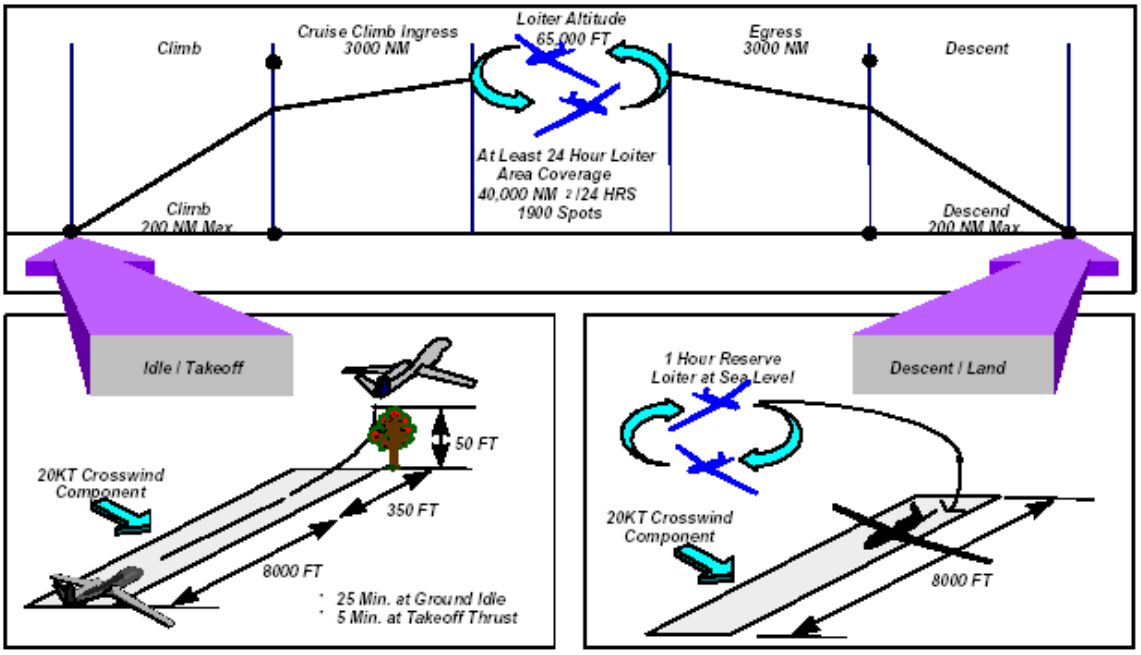

Fig. 2: Notional Global Hawk Mission Profile (8: 3-4)

In an attempt to keep changes to the proposed HALE UAV airframe to a minimum with the installation of the TIHE/Conventional Jet engine, no major modifications are made to the basic mission outline. The new mission profile will be split into two phases: the *conventional* takeoff, climb, and landing, along with the *TIHE-Powered* start at switchover altitude, climb to cruise condition, cruise to target area, long duration loiter, return cruise, and descent to switchover altitude.

Several important and overarching concerns should be addressed at this point. Obviously, the longer the vehicle is powered by the conventional engine, the more fuel

that is required. Minimization of the conventional engine run time must be weighed against operational requirements and safety issues. There would be significant political prohibitions on operating a high power gamma ray source like the TIHE engine near domestic, populated areas. Addressing this concern led to three main constraints on the mission development: restricting TIHE operation to a 20,000 ft (6.1 km) altitude deck, basing of operational units close to domestic or allied borders or oceans, and a 200 nmi conventional fly-out away from allied airspace. These constraints will be determined more by the political atmosphere than by any physical limitation and represent a best guess, which will have to be reevaluated at the time of actual design and operation of this proposed aircraft.

After the TIHE has become the primary power source for the engine, the mission loses its range limitations for the TIHE-cruise as well as the extended TIHE-loiter leg. The modified mission profile, shown in Fig. 3, shows only the ingress legs with the assumption that the egress will be a mirror image with the addition of the 1-hour SL conventional fuel reserve loiter leg. The variation in the three different mission profiles, shown in Fig. 3, is the altitude level at which the engine switches from conventional combustion to its Triggered Isomer heat exchanger mode. The switchover altitudes were chosen as 20, 30, and 40,000 ft (6.1, 9.14, 12.19 km) in order to study a parameter to optimize both conventional and TIHE phases.

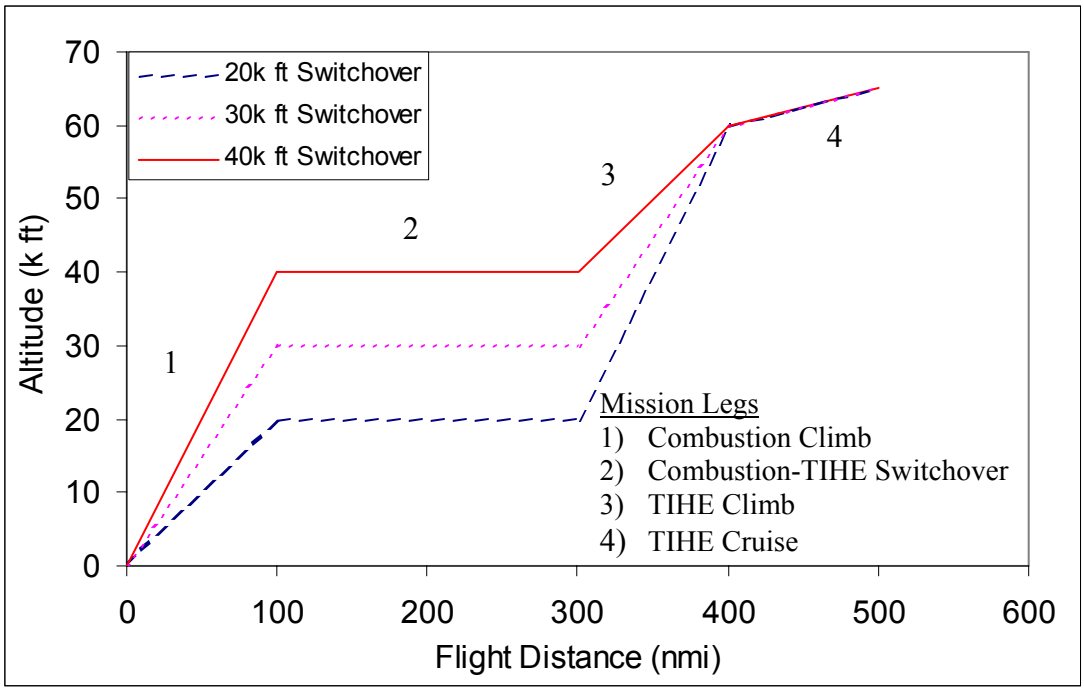

Fig. 3: **Proposed TIHE/Conventional Mission Profile**

3.4 Engine Selection

A major thrust of this research was to select the optimum engine type for use as a TIHE powered jet engine. Looking at a vast array of engine types allows for the selection of the best engine for the task. Several engine types were eliminated from study for the following reasons. Internal combustion engines were ruled out due to the inherent combustion reaction that will not be taking place with TIHE. Rockets may be an excellent choice for other applications of TIHE development. Propellant mass requirements during long duration atmospheric missions quickly become prohibitive due to large propellant weight. Ramjets and scramjets are also good choices of engines for other missions, but the subsonic flight regime utilized by the HALE UAV makes these engines inefficient compared to turbo machinery engines. Afterburning modifications to

turbo machine jet engines were not considered due to the mission requirement to minimize conventional fuel use. However, this modification could be looked at for increased maneuverability or for different missions.

Five engine types were examined: single spool turbojet, dual spool turbojet, split-stream turbofan, mixed-stream turbofan, and turboprop. No decision was made at the outset of this study to limit the aircraft to either a single hybrid engine or two or more completely separate engines.

3.5 Optimizing Switchover Altitude and Mach

The main variables in the TIHE/conventional HALE UAV mission, that were not initially decided, were switchover flight conditions. A major portion of the optimization process included determining an optimum altitude and Mach combination for switchover between the conventional phase of the mission and the TIHE phase of the mission. The method developed to determine this switchover condition was to use nine different switchover conditions. In this way, both a Mach sweep of 0.4, 0.5, and 0.6 along with an altitude sweep of 20 k, 30 k, and 40 k ft could be simulated. The max value of the Mach sweep was determined by the cruise Mach condition of the current Global Hawk mission.

3.6 AEDsys and ONX

Software that is based on the engine design methods described in Mattingly, Heiser, and Daley's *Aircraft Engine Design* textbook was used in the engine optimization

and selection process (16). Aircraft Engine Design System Analysis Software (AEDsys) version 2.13 (18) was used in conjunction with an embedded version of On-Design Analysis of Gas Turbine Engines (ONX) version 4.021 (19). ONX was used to develop a particular engine for on-design flight and this data was then saved into a data file for input into AEDsys. AEDsys was used to calculate fuel use and aircraft performance for the given on-design engine (from the ONX data file) and specific mission leg descriptions. It was also used to size inlet and exit areas for each of the inputted on-design engines. The following sections will describe how these two programs work together to calculate fuel consumption, thrust, and inlet and exit sizing for a given engine.

Both programs use a standard station numbering system that works for each type of jet engine. Figure 4 shows a diagram and a station-numbering scheme of a mixed stream turbofan engine and similar notation will be used for all types.

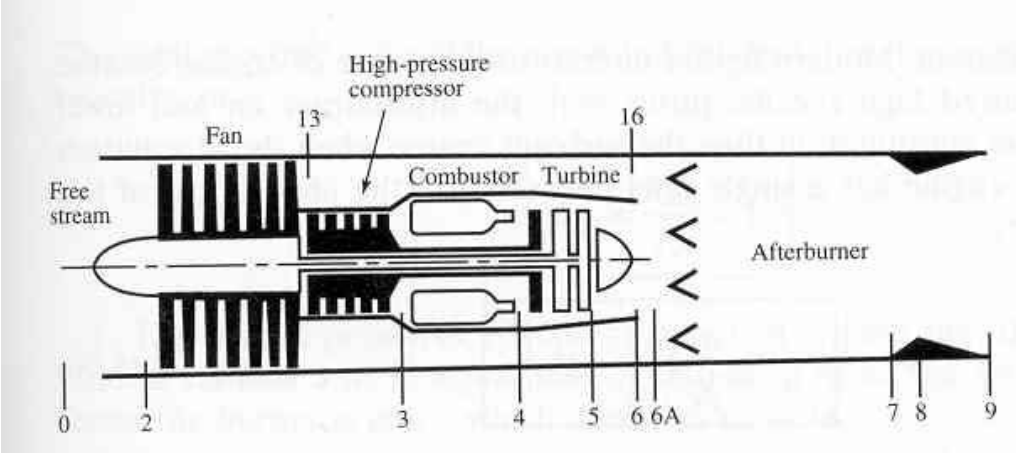

Station	Location	Station	Location
0	Free stream	4	Burner Exit
1	Inlet or diffuser entry	5	Turbine Exit
2	Fan Entry	9	Exhaust Nozzle exit
3	High Pressure Compressor (HPC) Exit	16	Bypass exit

Figure 4: Engine Station Numbering (source 20:313, image reproduced with permission from author)

3.6.1 ONX

ONX estimates engine performance parameters in terms of design limitations, flight conditions and design choices, by treating each stream in the engine as one-dimensional flow of a perfect gas. Non-ideal component behavior is accounted for by including realistic component efficiencies. (16:97) The process used is a fairly straightforward series of equations that calculate pressures and temperatures at each station, using the specified compressor pressure ratios, burner pressure ratio, turbine inlet temperature, mechanical efficiencies, and the efficiencies for diffusers, nozzles, burner, compressors, and turbines. These equations are specific for each engine type and utilize a work balance on the high and low pressure spools (if dual spooled) to determine the pressure and temperature ratios across the high and low pressure turbines. Equations that are not included in this document can be found in both *Aircraft Engine Design* and *Elements of Gas Turbine Propulsion* (16, 20).

One calculation of interest is the overall uninstalled thrust equation, which is the application of conservation of momentum to a control volume consisting of the flow entering and exiting the engine. In order to calculate the uninstalled thrust, eqn.(5) must have values for pressure, area, and velocity of the flow exiting the nozzle. These values are calculated as part of the ONX algorithm.

$$F = \frac{\left(m_9 V_9 - m_0 V_0\right)}{g_c} + A_9 \left(P_9 - P_0\right) \tag{5}$$

where

F = uninstalled Thrust (lbf)

m_0 = mass flow rate at station (lbm/sec)

V = velocity at station (ft/sec)

A = cross-sectional area (ft^2)

g_c = Newton's constant (32.174 lbm ft/(lbf sec^2))

Since mass flow rate, m_0, is not an input to ONX, the program tabulates its results as specific values such as specific thrust (F/m_0) and uninstalled thrust specific fuel consumption (S). These values along with fuel-to-air ratio, ONX input values, component pressure ratios, and component temperature ratios are saved to the output reference file. Immediately prior to saving the reference file, the software requests a reference mass flow rate and calculates the thrust and fuel consumption rates at the on-design condition.

This process of creating an engine in ONX is very fast, once all of the input values have been determined. A large series of engines at different on-design values can be created rapidly with small incremental changes of any of the 20+ inputs. To be effective in an optimization study, many of the inputs are chosen to be constant, in order to reduce the search to a reasonable time limit. This calls for finding the best combination of a few of these parameters while using realistic estimates for the other input values.

Each engine type utilizes slightly different input parameters, however many of the component parameters are similar in all engine types. These similar values that were set constant for this study have been collected in Table 1.

Table 1: Engine Design Parameters

Description	Design Value	Description	Design Value
Polytropic Efficiency		*Total Pressure Ratio*	
Fan	0.89	Inlet	0.97
Low Pressure Compressor	0.89	Burner	0.97
High Pressure Compressor	0.9	Mixer	0.97
High Pressure Turbine	0.89	Nozzle	0.98
Low Pressure Turbine	0.91	Diffuser Max	0.97
Component Efficiency		*Miscellaneous*	
Burner	0.98	Fuel (JP-4) Heating Value	18000 BTU/lbm
Mechanical		Turbine cooling air	5%
Low Pressure Spool	0.99	Bleed air flow	1%
High Pressure Spool	0.98	Power take off	1%
Power Takeoff	0.98	P0/P9	1
Propeller	0.82	Mach Number @ 6	0.4
Propeller Gear	0.99		
Component Specific Heats		*Ratio of Specific Heats*	
Compressor	.238 BTU/lbm-R	Compressor	1.4
Turbine	.295 BTU/lbm-R	Turbine	1.3

This now leaves only a few very important design choices to be studied for the optimization process. At this point, material and structural limitations are looked at in order to set engine control values for AEDsys to limit engine operation.

3.6.2 Engine Controls

Several maximum parametric values are important in both the ONX and AEDsys programs. AEDsys, in particular, uses these inputs as engine controls and restricts the engine from operating above these values. Due to the first-order optimization of several engine types in this study, general values were sought for ease of use to be applied across all engine types. A more comprehensive engine design would yield more accurate engine control values, however this would normally be done at a later stage of engine design. In this section, methods to select these values will be described.

By noticing trends in values of current and future engines, many realistic choices can be made (21, 22). For turbine inlet temperature (T_{T4}), a 3200 °R (1778 K) maximum value was selected consistent with values for current engines. Maximum overall compressor ratio (π_c) was chosen to be 35, to coincide with current technology. The maximum value for compressor exit temperature (T_{T3}) was chosen by the same methods at 1600 °R (889 K). This value is slightly higher than current engines and accounts for advances in material temperature tolerances. Values for maximum speed for the spools were set at 105% of reference RPMs. The final control value needed to be examined a little more rigorously.

The maximum compressor pressure (P_{T3}) limit was calculated using hoop stress theory. This method calculates the maximum internal pressure that a hoop of a specific material, of a chosen thickness and radius, can withstand without yielding or failing. An equation that calculates the maximum allowable pressure inside of a hoop of a specific thickness follows:

$$P_{max} = \frac{\sigma_Y \, d}{r} \tag{6}$$

where

P_{max} = Maximum Internal Pressure (psi)

σ_Y = Yield Stress (psi)

d = thickness of hoop (in)

r = radius of hoop (in)

Assuming that titanium or a titanium alloy is used in the construction of the engine cowling, yield stress varies from 20 – 145 kpsi (136-1000 MPa), depending on the specific alloy (23). To ensure safety, the lower value of yield stress was used for calculating maximum Pt3. A 2-ft diameter engine cowling (r = 1 ft), with ¼-in thick casing was used as the reference conditions, with the understanding that if the diameter increased, the thickness of the cowling would have to increase to compensate. This, in turn, allows for a constant max P_{T3} value regardless of engine diameter. These values inputted into eqn. (6) result in a max P_{T3} value of 410 psi (2.83 MPa). For added safety, 90% of this value was used, setting the max P_{T3} control at 370 psi (2.55 MPa). This value is close to other existing engine values and was deemed appropriate for this study.

3.6.3 Off-Design Analysis

Imbedded in the mission analysis algorithm of AEDsys is a sub-algorithm that estimates an engine's performance over its operating envelope. This process differs significantly from the on-design calculations, where all of the design choices are free to be chosen in order to achieve ideal specific thrust (F/m_0) and thrust specific fuel

consumption (S) values for a design condition. The off-design subroutine uses an iterative method, since the design choices have been made previously in ONX and the performance of the inputted specific design point engine is needed at all possible operating conditions. This indirect method solves a set of independent equations, in order to solve for an equal number of dependent variables. Two important concepts are mentioned here to help explain this off-design analysis method (16).

The first is called referencing, in which conservation of mass, momentum, energy, and entropy are applied to the one-dimensional steady flow of a perfect gas at either an on-design or off-design steady state operating point. This leads to relations between temperature and pressure ratios that apply to both operating points and can be applied to utilize the reference values from the on-design analysis to calculate the off-design parameters.

The second concept employs a mass flow parameter, where the one-dimensional area specific mass flow property is written in terms of total pressure, total temperature or Mach number. This technique is useful in applying the conservation of mass equation and in calculating flow areas.

Another important aspect of the off-design subroutine is that it not only calculates full thrust values at off-design conditions, but it allows throttling the thrust through fuel control to any thrust level within its operational limits. These off-design analysis methods and related equations are described in detail in Mattingly's text (16) and are not included in this document.

3.6.4 Flight Performance Analysis

The most important aspect of AEDsys is that it calculates required thrust and corresponding thrust specific fuel consumption for each mission leg by taking into account the off-design performance of a chosen engine, the aerodynamic forces applied on the aircraft during the leg, and the changing weight of the aircraft due to fuel consumption. The off-design method was discussed previously. In this section, the changing weight issues and the aerodynamic forces are discussed.

Weight change in an aircraft is usually due to fuel consumption and releasing stores or disposable items. For studying the HALE-UAV mission, this weight change rate is equal to the fuel consumption rate:

$$\frac{dW}{dt} = -TSFC\ T \tag{7}$$

where

W = weight (lbf)

TSFC = installed thrust specific fuel consumption (lbm/(lbf sec))

T = installed thrust (lbf)

The T and TSFC values are not the same as the uninstalled F and S values calculated by ONX and the off-design subroutine. The installed thrust value will be smaller and TSFC larger, due to losses added by the inlet and exit nozzle for an installed engine. TSFC can be calculated by incorporating a loss model that can determine the uninstalled thrust needed to attain the required installed thrust. This issue will be addressed when engine sizing is discussed in section 3.7.

Since T values are needed for both weight change calculations and the off-design subroutine, a discussion of flight dynamics is required. The basic forces involved in flight were described in section 3.1. Several important related terms need to be determined for use in later calculations.

In order to calculate aircraft flight performance, two important terms must be calculated or chosen. The first term is called takeoff thrust loading (T_{SL}/W_{TO}) and is simply the ratio of takeoff thrust (sea level static) to takeoff weight. The second is called wing loading (W_{TO}/S) and is the ratio of takeoff weight to wing surface area. In this study, T_{SL}, W_{TO}, and S have been set as the Global Hawk reference values. Since the goal of this study is to replace the current propulsion system with the TIHE/Conventional system and not to make major modifications to the aircraft structure, these values were set constant to T_{SL} = 8294 lbf (36.9 kN), W_{TO} = 25600 lbf (113.9 kN) and S = 540 ft^2 (50.17 m^2). (26; 9) With these values set, thrust loading and wing loading were set at values of T_{SL}/W_{TO} = 0.324 and W_{TO}/S = 47.4 lbf/ft^2. These values were used in various versions of the flight performance equation that AEDsys uses for its calculations.

This flight performance equation is constructed by using the principle of conservation of energy around the aircraft. It sets the rate of mechanical energy input equal to the rate of change of potential energy and kinetic energy. The full flight performance equation (8) used in AEDsys assumes that thrust and aerodynamic drag act in the same direction as the velocity.

$$\frac{T-(D+R)}{W}V = \frac{d}{dt}\left(h + \frac{V^2}{2\,g_0}\right) \tag{8}$$

where

D + R = total air resistance (lbf)

V = velocity (ft/sec)

h = altitude (ft)

g_0 = acceleration of gravity (ft/sec^2)

t = time (sec)

The left hand side of the equation represents the mechanical power delivered into the system. The right hand side is also known as the weight specific excess power or P_s and is the time derivative of the sum of the aircraft's kinetic and potential energies. AEDsys breaks each mission leg into two distinct categories based on its P_s value. The first case is when there is increasing P_s and is characterized by known values of altitude and velocity changes and usually requires full thrust from the engine at the flight conditions specified. Combining eqns (7) and (8) along with an integration, results in the P_s>0 weight fraction equation:

$$\Pi_i = e^{\left(\frac{-TSFC}{V\left(1-\frac{D+R}{T}\right)}\Delta\left(h+\frac{V^2}{2\,g_0}\right)\right)} \tag{9}$$

where

Π_i = weight fraction ($W_{final}/W_{initial}$)

Δ = Change in value from initial point to final point

This value of Π_i represents the percentage change in weight that occurs during a mission leg. In order to calculate the total aircraft weight after a mission leg, all previous weight fractions, including the current mission leg's value, are multiplied together with the takeoff weight of the aircraft.

The second case is when $P_s = 0$, and represents mission legs where altitude and velocity are known as well as time duration or range distance. These legs usually utilize less than full thrust from the engine and require the throttling method used in the off-design subroutine. In this case, thrust will equal the total drag on the aircraft. The following flight performance equation is used by AEDsys for these mission legs

$$\Pi_i = e^{-TSFC\left(\frac{D+R}{W}\right)\Delta t} \tag{10}$$

One last concept to understand with these weight fraction equations (eqns (9) & (10)) is that due to the integration involved, the values within the equations can change significantly over a mission leg, leading to erroneous results. The most common method to combat this problem is to break up long mission legs into several smaller legs and use better average values for the smaller segments. This results in a better value for fuel consumption than a single averaged equation, but takes less computing time than a full blown numerical integration. This method was used in both of the 200 nmi switchover legs.

3.7 Engine Sizing

Inlet and exit nozzle sizing has direct impact in not only mass flow rates through an engine, but also on calculating installation drag losses. Since the aircraft drag analysis

did not include any losses from the engine, engine sizing is where this loss is taken into account. The off-design algorithm in conjunction with the mission analysis subroutine calculates the maximum required choked freestream area (A_0*) and nozzle exit area (A_9) for each mission leg in two ways: a constant loss model and a size based drag loss model.

The first method assumes a constant loss of .0909 or roughly 9%, due to the engine. This becomes the difference between installed thrust and uninstalled thrust, with installed thrust being about 91% of the uninstalled thrust. This value, which is a rough first order estimate, was used in a first iteration in the engine sizing method.

Once values of A_0* and A_9 are calculated by AEDsys using the 9% loss model, the largest values of these are used for sizing the inlet and exit nozzles. For the inlet area (A_1), it must be slightly larger than the area that would cause the flow to choke, therefore, since the aircraft only flies at subsonic speeds, the inlet choke area (A_1*) is equal to A_0*. An equation that calculates the critical area ratio that causes an isentropic flow to attain Mach 1.0, eqn (11) allows for the calculation of the inlet area

$$\frac{A_1}{A'_1} = \frac{1}{M_1}\left[\frac{2}{(\gamma+1)}\left(1+\frac{\gamma-1}{2}M_1^{\,2}\right)\right]^{\frac{\gamma+1}{2(\gamma-1)}} \tag{11}$$

where

A'_1 = choked inlet area, also A_1^* and A_0^*

M_1 = Mach number at inlet

γ = ratio of specific heats

Once a value for the A_1/A_1^* ratio has been calculated, a safety margin of 4% is included to ensure the inlet area will not choke the flow. This gives a calculation for the inlet area needed for an engine with a 9% loss from F to T.

$$A_{1design} = 1.04 \left[\frac{A_1}{A'_1} \right] A0' \tag{12}$$

For exhaust nozzle sizing, it is required that the size must not be smaller than the largest value required throughout the flight. A ten percent safety factor is multiplied to the largest A_9 value to calculate the engine exit area (A_{10}). A simple method derived from current trends in exit nozzle geometry is used to calculate the length (l) of the nozzle based on A_{10}. (16:203)

$$l = 1.8 \sqrt{\frac{4A_{10}}{\pi}} \tag{13}$$

Once these three engine-sizing values were calculated based on the 9% loss model, a second iteration of AEDsys was run to get more accurate losses. This next iteration utilized the second method, used in the AEDsys program, for installed engine losses: the size based drag loss method. The inlet loss model utilizes conservation of mass and perfect gas isentropic relations to calculate the drag losses caused by the inlet. Methods for determining exit nozzle losses are not as straight forward and a correlation method has been developed based on experimental testing. This method utilizes the exit nozzle geometry values of A_{10}, D and freestream Mach number. Both of these methods are developed in chapter 6 of *Aircraft Engine Design* (16).

3.8 Conventional Engine Selection Method

With nine different flight conditions set from the switchover Mach and altitude test values, along with the five different engine types, 45 engine optimizations were scheduled. Each optimization was based mainly on the engine type and will be explained later. One parameter, T_{T4}, was modified to minimize fuel consumption in the conventional engines in early runs but due to low sensitivity shown as well as run time and input issues, its value was not modified in the ONX program. It was subsequently set at a constant 3200 °R for the optimization runs.

An engine naming convention was created to easily identify the engine created by ONX for use in the AEDsys program. Each engine was given a series of letter designators to differentiate type: tjs for single spool turbojet, tj for dual spool turbojet, tfs for split stream turbofan, tfm for mixed stream turbofan, and tp for turboprop, as well as numerical designators for switchover Mach number and altitude. For example, tfm5304 would represent the fourth turbofan mixed stream engine created for the Mach 0.5, 30,000 ft switchover conventional mission.

The chosen optimization method utilized an engine selection process that involved ONX, AEDsys, and off line Excel spreadsheets that aided in the calculating engine size and tabulated results. The method was similar for all engines tested and in all switchover missions. An initial design point was inputted into ONX and an ONX reference file was produced. This file was brought up into the specific switchover mission in AEDsys. The engine control values calculated earlier in section 3.6.2 were entered and a 9% loss model was selected. The Mission Analysis routine was run to calculate engine performance at each leg of the mission. With the completion of each

leg, the mission summary presented values of max A_0^*, A_9, and total fuel consumption. The largest values were recorded and inlet and exit geometry was calculated, outside AEDsys, using the methods described previously. The new values for A_1, A_{10}, and l were inputted into the loss model calculator to be run concurrently with the mission and off-design algorithms. This second run produced a value for fuel consumed for the entire conventional mission. This value was recorded and work began on the next on-design engine to be tested.

One test parameter was increased by a small percentage while leaving the rest of the test parameters constant. This new engine was saved as an ONX reference file with a designator of the next sequential number. The above method of running AEDsys first, with the constant loss model to find sizing, and then with the size dependant loss model for better accuracy, was used. This resulted in a fuel-consumed value for the new engine. This fuel consumption value was compared to the previous value and if the change to the test parameter caused a decrease in total fuel consumed by more than 10 lbf, the parameter was changed by an additional increment in the same direction either positive or negative.

If the change to the test parameter increased fuel consumption, the test parameter was decreased by a similar percentage and saved as a new ONX reference engine file. Again this engine was run for the mission to calculate total fuel consumption. If this engine showed lower fuel consumption by 10 lbs or more, the next iteration would decrease the test parameter another increment. This process was continued until no significant decrease in fuel consumption could be gained.

During this process, AEDsys also checks to see if the engine can operate at the flight conditions and engine control limits prescribed. If the engine fails to operate at any leg during the mission or it is unable to provide significant thrust, it is treated as if it increased fuel consumption. In some cases, the windows for different test parameters that a specific engine could operate in were very small.

This engine selection process was used for each engine type. The first engine tested was the single spool turbojet. The variables that were examined to optimize this engine were on-design free stream Mach number (M_0), altitude (h), and compressor pressure ratio (π_C). The dual spool turbojet's test variables were M_0, h, π_C, and low-pressure compressor pressure ratio (LPC π). The split stream and mixed stream turbofan's test variables were M_0, h, π_C, bypass ratio (α), and fan compressor pressure ratio (πC'). The turboprop test variables were M_0, h, π_C, and turbine temperature ratio (τ_T).

These optimization runs normally produced between 10 and 20 engines, culminating in an optimized engine for its type and switchover flight conditions. The first optimization runs tended to take longer to converge to an engine selection, however once an engine was selected for the first flight condition, it was used as a baseline for the next flight condition. For example, the single spool TJ selected for the Mach 0.4, 20,000 ft switchover was chosen as the baseline engine for the Mach 0.4, 30,000 ft case. The two turbofan engine optimization runs also tended to be longer due to the increased number of test parameters.

At the end of this conventional engine optimization process, 45 engines were selected as the optimized engines of their type and flight conditions. It was hoped that

from these engines a most efficient altitude, Mach number, and engine type could be selected for the conventional portion of the mission. Other considerations, such as engine size, would be secondary selection criteria to be looked at after the results of the TIHE portion of the mission were analyzed.

3.9 TIHE engine selection process

Engine selection criteria for the TIHE powered engine were different than those used for the conventional mission, since fuel consumption of the isomer would be negligible. A method to determine selection criteria had to be developed. Since the flight of the TIHE engine would take place at medium and high altitudes, it was conceivable that some engine types would be significantly less efficient than others. So the ability of an engine to operate and provide sufficient thrust at all TIHE mission flight conditions was of primary importance.

Power requirements were determined to be the secondary factor in TIHE engine selection. Since radiation-shielding weights are directly affected by power output from the heat source, the engine that required the smallest heat power would be considered the optimum choice.

Due to AEDsys' ability to calculate important flight and engine parameters quickly through a mission, it was decided to also use this software package for the TIHE engine selection process. A means for calculating heat power required was developed from the outputs provided by AEDsys as follows. Since the conventional fuel provides all of the heat into the conventional system, it is possible to calculate the heat power

required to run the TIHE system as though it were a conventional engine at the specific TIHE flight conditions.

AEDsys provides T and TSFC values at each mission leg, multiplying these values together results in a fuel consumption rate.

$$m_{fdot} = T \cdot TSFC \tag{14}$$

where m_{fdot} is the fuel consumption rate (lbm/sec.) Fuel consumption rate, along with the burner efficiency value, which represents the ratio of heat energy rise actually supplied to the system to the maximum heat power possible, and the heating value of the fuel, can be used to calculate the heat power required by the TIHE.

$$Q_{burner} = \eta_b \, h_{pr} \, m_{fdot} \tag{15}$$

where

Q_{burner} = heat power required by TIHE (BTU/sec)
η_b = burner efficiency
h_{pr} = heating value of fuel (BTU/lbm)

Equations (14) and (15), along with outputs from AEDsys, allow the calculation of required power at all points along the TIHE powered portion of the mission. Thus creating valid and important criteria for the selection process.

Since low fuel consumption rates were essential for both the conventional engine selection and TIHE engine selection, it was deemed that utilizing the same engines that were selected for the conventional missions, for the TIHE engine selection process would

be prudent. At this point, it becomes important to note, this choice does not represent a decision to use a single engine for both missions.

Engines, selected for the conventional mission for a particular switchover Mach and altitude, used for the TIHE legs, had to begin at that switchover flight condition. This limits the study, in that engines, run from 20 k ft to 65 k ft, cannot be directly compared to the TIHE engines that run from 40 k ft to 65 k ft, for all mission legs. Since the loiter/cruise conditions at the peak of the TIHE climb (Mach 0.6, 60,000 ft) were the same for all engines, the required power at this point is directly comparable between different engines (see Table 2). Therefore, this cruise required power was another important figure of merit.

Table 2: Mach number for TIHE climb schedule for each switchover flight condition

Altitude	Mach 0.4 20 k ft	Mach 0.4 30 k ft	Mach 0.4 40 k ft	Mach 0.5 20 k ft	Mach 0.5 20 k ft	Mach 0.5 20 k ft
20	0.400			0.500		
25	0.425			0.513		
30	0.450	0.400		0.525	0.500	
35	0.475	0.433		0.538	0.517	
40	0.500	0.467	0.400	0.550	0.533	0.500
45	0.525	0.500	0.450	0.563	0.550	0.525
50	0.550	0.533	0.500	0.575	0.567	0.550
55	0.575	0.567	0.550	0.588	0.583	0.575
60	0.600	0.600	0.600	0.600	0.600	0.600

In order to run the TIHE engine in AEDsys, the program had to be manipulated into not burning any fuel while still calculating fuel consumption rates. Setting distance and time lengths for each point in the climb to zero accomplished this. Also, since the goal of the TIHE engine optimization was to compare engines as closely as possible, a flying weight of the aircraft had to be set. A value of 20,000 lbf (88.9 kN) was used as

the weight of the aircraft after the conventional portion of the flight burned fuel. This value was used due to the assumption that the takeoff weight of the aircraft would remain 25,600 lbf and that approximately 5000 lb (22.2 kN) of fuel would be consumed, or that if less fuel was consumed by more efficient engines, the takeoff weight would be reduced accordingly.

3.10 Triggered Isomer Decay

The USAF Air Force Office of Scientific Research (AFOSR) has been sponsoring an international group of physicists to research an exciting new process for extracting energy from isomers of Lutetium (Lu), Hafnium (Hf), and Tantalum (Ta). These 4 and 5-quasiparticle isomers of Lu, Hf, and Ta are being examined because they are hindered from spontaneous radiative decay due to their specific structural composition. This causes the 2 to 3 MeV excited states of these isomers to have relatively long lifetimes. The process of extracting energy consists of bombarding the isomer with X-rays to excite the material to a higher energy state that would release the nucleus from its structural prohibitions. A rapid decay of the excited isomer could release the total energy of the isomer plus that of the absorbed trigger photon. (4:695; 5:2-13)

In particular, the researchers have focused on the 31-year half-life, 4-quasiparticle isomer ^{178}Hf with a 2.446 MeV excitation energy. Using 10 to 90 keV X-ray pulses from a dental-quality device, they were able to cause the absorption of X-ray photons on the order of 40 keV of energy to induce the prompt release of the 2.446 MeV stored in the hafnium isomer. The results of this research lead to a source of power that returns 60 times the energy inputted into the isomer from the X-ray. In particular, the ^{178}Hf isomer

stores approximately 1.3 GJ/g of energy and with this X-ray triggered accelerated decay and volumetric energy release rates of up to 50 GW/m^3 are possible (5).

This reaction differs from fission reactions in that while there is significant gamma ray radiation (<600 keV), there is no significant neutron release. (4: 697; 5: 2-14.) This process becomes attractive because the energy release is on the order of 1% of that released from fission reactions, while producing no neutrons or fission products. This becomes important when considering shielding and disposal concerns, because shielding weight drops and maintenance and removal of used fuel becomes much safer.

3.11 Radiation Shielding

There are three means to minimize radiation dosage on people and on materials: exposure time, distance, and shielding. For application in a HALE UAV, exposure time will be high and distance will be minimized to keep the airframe small. This leaves shielding as the critical element to protection of electronic equipment and sensors.

Since the highest level of radiation will be in the form of 600keV gamma rays, this leads to a straight forward method to determine shielding weights. The method utilized for this study is derived from a procedure developed in Turner's textbook *Atoms, Radiation, and Radiation Protection* (24: 452-456).

Treating the Hafnium reactor as a point source of gamma rays, an unshielded exposure rate can be calculated. Prior to ONX and AEDsys runs, an initial estimate of heat power output required by the TIHE of 5 MW was used. Efficiency requirements of the heat exchanger will require that most of the radiation will be contained, leaving

approximately 5% of the heat power output as escaping radiation. (6: 2-13; 5: 2) The intensity of radiation at a specified distance from a gamma source, neglecting attenuation in air, can be calculated by (24: 368):

$$\Psi = \frac{CE}{4 \pi r^2} \tag{16}$$

where

Ψ = Intensity or energy fluence rate (W/m^2)
CE = Radiation output at source (W)
r = Distance from source (m)

Gamma photons traveling through matter are governed statistically by an interaction probability per unit distance traveled. This interaction probability is referred to as the linear attenuation coefficient μ and has units of inverse length (cm^{-1}). This value depends on the medium that the photon travels in and the energy level of the photon. A more widely used parameter is called the mass attenuation coefficient μ/ρ in units of cm^2/g and represents the probability of an interaction per g/cm^2.

Of these interactions, matter has a statistical chance to absorb the photon and therefore absorb the energy. This probability of energy absorption called the mass energy-absorption coefficient μ_{en}/ρ is also in units of cm^2/g. The mass energy-absorption coefficient of photons with energies between 60 keV and 2 MeV traveling through air is approximately constant at .027 cm^2/g (.0027 m^2/kg) (24: 194). These concepts lead to an equation to calculate dosage of gamma radiation through air:

$$D_{rad} = \Psi \left[\frac{\mu_{en}}{\rho} \right] \tag{17}$$

where

D_{rad} = Radiation Dose (W/kg)

Ψ = Intensity or energy fluence rate (W/m^2)

μ_{en}/ρ = mass energy absorption coefficient (m^2/kg)

With our initial estimate of 5 MW as the total heat power generated, there will be 250 kW of radiation output from the source. Using eqn. (16) with a distance of 3 m, an intensity of 2210 W/m^2 is calculated. Using the 0.0027 m^2/kg value for the mass energy absorption coefficient, eqn. (17) results in a radiation dose of 5.968 W/kg or 596.8 rad/sec.

The next step in determining shielding requirements is to determine radiation dose tolerance levels for equipment. Tolerances for electronics vary widely. By assuming that equipment on board the HALE UAV can be hardened to space application levels gives a target dose tolerance of .01 to 2 rad/sec levels. (25)

Another factor to consider in shielding requirements is that the scattering of photons from matter interactions can cause a higher intensity of radiation than that just from direct rays (see Fig. 5). This increased intensity can be accounted for by including a buildup factor into the equations for determining required shield thickness. Buildup factors (B) can be obtained from calculations or measurements for given shield material, thickness, source geometry, and photon energy.

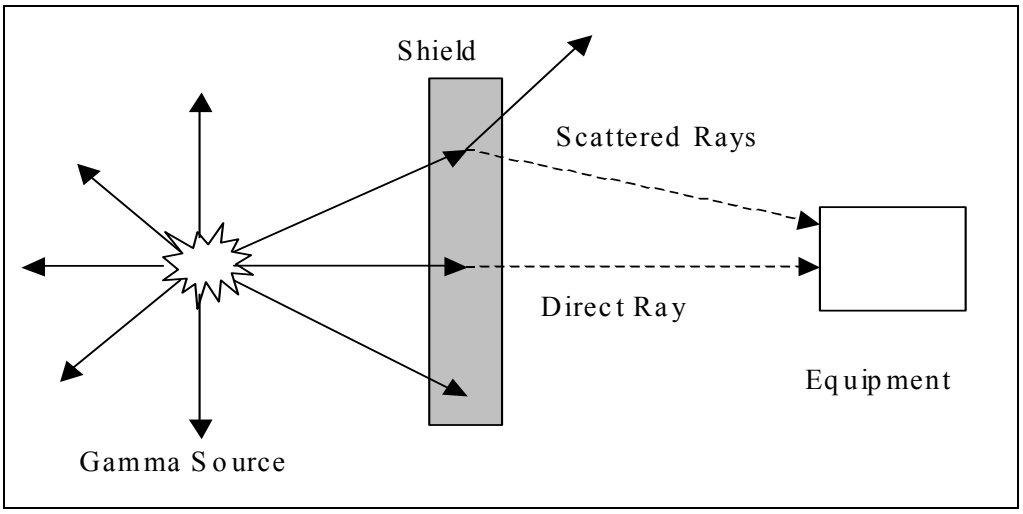

Fig. 5: Gamma Ray Scattering

Normally, the thickness of shielding is the parameter being searched for so an iterative method can be used to determine both the buildup factor and shield thickness. An equation that calculates the shield thickness required for an isotropic point source is:

$$I = I_0 \cdot B \cdot e^{-\mu x} \tag{18}$$

where

I = Intensity at target with shield (rad/sec)

I_0 = Intensity at target unshielded (rad/sec)

B = Dose buildup factor

μx = relaxation length

Starting with the assumptions that the maximum energy state for gamma rays escaping the core are at the 500 keV range and that Lead is used as the shielding material, the iterative process begins with assuming a dose buildup factor of 1 and solving for the

relaxation length μx. Once a solution for the relaxation length has been made from the buildup factor equal to 1, a new value for B can be determined from a chart of dose buildup factors vs. relaxation length (see Fig. 6).

Fig. 6: Dose Build up Factor for Point Isotropic Source of 500 keV photons in Lead (Source: Table 15.1, 24: 452)

The values of B and μx will converge after a few iterations. In the analysis so far, values were determined for I of .01 rad/sec and for $I_{0,}$ which is equal to the radiation dose, of 596.8 rad/sec. The iterative method results in a Dose Build up factor of 2.445 and a relaxation length of 11.891. The following equation can be used to back out a value for the shielding thickness required:

$$x_{lead} = \frac{\mu x_{lead}}{\left[\frac{\mu}{\rho}\right] \rho_{lead}} \qquad (19)$$

where

x_{lead} = Shield thickness (cm)

μx_{lead} = Relaxation length

μ/ρ = Mass Attenuation Coefficient (cm^2/g)

Using a value for the mass attenuation coefficient of lead for photon energy values of 500 keV (7:187) is .15 cm^2/g and that along with the density of Lead of 11.4 g/cm^3 results in a shield thickness of 6.95 cm.

The next step in shielding requirements is determining the total weight of shielding. A useful value for shielding is called shield loading and is simply the shield thickness multiplied by the density of the shielding material. With the shield thickness calculated above of approximately 7 cm, the shield loading would be 793 kg/m^2. Shield loading multiplied by the surface area of the proposed shield will result in the total shield weight. A sphere is normally the ideal shape of shielding due to minimum surface area. A quick look at the area of a sphere:

$$A = 4 \pi r^2 \tag{20}$$

where

A = Shield area (m^2)

r = Radius of Sphere (m)

This equation along with shield loading can be used to show how quickly shield weight will increase with small increases in shield distance from source. Figure 7 shows that for a vehicle in the 25,000 lbf (111.2 kN) total weight class, any shield distance of

more than about a meter causes the shield weight to become close to the total weight of the aircraft. This requires placing the shield as close to the source as possible. Luckily, a gamma ray shield can be placed anywhere between the source and the equipment to be protected (24: 455) so we are only limited by structural constraints.

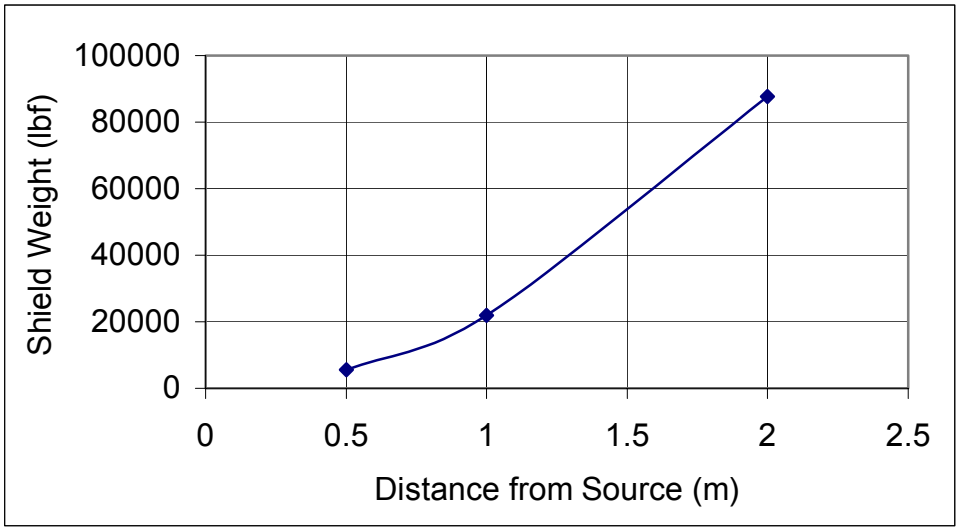

Figure 7: Shield weight sensitivity to shield distance

The concept of divided shielding used during the research of the ANP/NEPA programs could be utilized to reduce total shielding requirements. To utilize this technique a detailed study of placement of equipment in the airframe would be required. For the scope of this research, the technique used to reduce shielding weight will be to use a semi-spherical shield. Due to the proposed location of the isomer reactor within the engine cowling, this semi sphere will give protection to the majority of the aircraft while allowing radiation escape to the aft and top of the aircraft. Assuming that we can place the semi sphere shield at a distance of 0.5 m from the source this leads to a shield weight

of 2743 lbf (12.2 kN). This represents only 11% of our reference take off weight for our HALE UAV or 19% of the fuel weight of the conventional Global Hawk aircraft.

3.12 TIHE Weight and Fuel Calculations

While shielding weight is most likely going to be the critical factor in the feasibility of using a TIHE source for a jet engine, other weights will need to be considered for completeness. The two topics covered in this section will be the weight of the Heat Exchanger itself and the required isomer fuel to power the Heat exchanger.

Calculating heat exchanger weight is a complex and time-consuming project. Fluid flow factors such as heat transfer, viscosity, and turbulence must be included in any attempt at designing heat exchangers and therefore requires rigorous computational models or extensive experimental work. Preliminary research on TIHE was discussed in Chapter 2 and will provide the background for the weight values used in this study.

Due to the variety of materials and geometries that could be used for the TIHE, weights vary from 800 lbf to 1200 lbf (365 kg - 560 kg) (6: 4-16). The assumption used for these values were that they could power a jet engine to provide 8-10,000 lbf of thrust and fit within the combustor section of the engine without intensive modification. While the thrust provided is approximately 10 times higher than that expected to be necessary for the proposed mission legs, it seems prudent to utilize these values in the current study. Methods could be developed to create thrust-to-weight correlations for TIHEs, however with only one study to consult, the decision was made to use the values from the Hartsfield's research (6).

For the actual hafnium material to be utilized as the isomer energy source, weight calculations could be made in a straightforward manner. With values of required power, duration of use, efficiency, and energy stored: an equation of fuel mass required can be derived

$$m_{hafnium} = \frac{Q_{required} \Delta t}{e_{stored} \varepsilon_{heat}} \tag{21}$$

where

$m_{hafnium}$ = mass of hafnium required (kg)
$Q_{required}$ = heat required power (W)
e_{stored} = mass specific energy stored (W/kg)
ε_{heat} = heat conversion efficiency

A sample calculation using the values determined in previous sections, of $Q_{required}$ of 5 MW and e_{stored} of 1.3 GJ/g, along with a value of ε_{heat} of 10%, estimated from efficiency values of fission reactors tested in the NEPA/ANP programs and Soviet nuclear programs (26: 147; 1: 26), result in a mass of about 24 kg. This value represents a minimum value of isomer fuel needed to provide the required heat power into the system. If the hafnium fuel is made part of the heat exchanger structure as proposed (6), this weight will be incorporated by the heat exchanger weight.

4. Results

4.1 Assumptions

In order to proceed with the daunting task of optimizing and comparing such a large number of different engine types, several assumptions were made.

1. A controlled triggered decay of hafnium isomers can be developed to the point that a compact heat source can be produced.

2. Triggered isomer heat exchangers can produce equal heating rates to chemical combustors and be of similar size.

3. Flight of the TI source will be allowed, with constraints that will restrict the operation of the source below 20,000 ft altitude.

4. Structural changes necessary for the addition of the shield, triggering mechanism, a possible second engine, and other modifications will not radically alter the drag polar of the aircraft.

4.2 Conventional Engine Results

The optimization of the nine switchover choices ended with some clear trends in efficiency in all three categories: switchover Mach, switchover altitude, and engine type. Complete results are listed on the following pages in Table 3 and Fig. 8.

Table 3: Fuel consumption values for switchover optimized engines

Engine Type	Engine Designation	Fuel Consumed (lbf)
Mach .4		
20000ft changeover		
turbojet 1spool	tjs4206	4475
turbojet 2spool	tj4209	4380
Turbofan Split Stream	tfs4214	3072
Turbofan Mixed Stream	tfm4213	3608
Turboprop	tp4214	1645
30000 ft changeover		
turbojet 1spool	tjs4206	3997
turbojet 2spool	tj4300	3937
Turbofan Split Stream	tfs4307	2725
Turbofan Mixed Stream	tfm4213	3225
Turboprop	tp4306	1430
40000ft changeover		
turbojet 1spool	tjs4402	3967
turbojet 2spool	tj4303	3931
Turbofan Split Stream	tfs4405	2671
Turbofan Mixed Stream	tfm4407	3146
Turboprop	tp4404	1588
Mach .5		
20000ft changeover		
turbojet 1spool	tjs5206	5060
turbojet 2spool	tj5209	5104
Turbofan Split Stream	tfs5200	3787
Turbofan Mixed Stream	tfm5210	3900
Turboprop	tp5209	3097
30000 ft changeover		
turbojet 1spool	tjs5303	4320
turbojet 2spool	tj5308	4252
Turbofan Split Stream	TFS5311	3106
Turbofan Mixed Stream	tfm5310	2957
Turboprop	tp5316	2607
40000ft changeover		
turbojet 1spool	tjs5408	3864
turbojet 2spool	tj5403	3883
Turbofan Split Stream	tfs5422	2542
Turbofan Mixed Stream	tfm5407	2603
Turboprop	tp5413	2067

Engine Type	Engine Designation	Fuel Consumed (lbf)
Mach .6		
20000ft changeover		
turbojet 1spool	tjs6206	6585
turbojet 2spool	tj6210	6525
Turbofan Split Stream	tfs6200	4936
Turbofan Mixed Stream	tfm6214	4785
Turboprop	tp6202	6406
30000 ft changeover		
turbojet 1spool	tjs6300	5138
turbojet 2spool	tj6305	5085
Turbofan Split Stream	tfs6307	3832
Turbofan Mixed Stream	tfm6309	3803
Turboprop	tp6308	4943
40000ft changeover		
turbojet 1spool	tjs6405	4278
turbojet 2spool	tj6403	4230
Turbofan Split Stream	tfs6408	3144
Turbofan Mixed Stream	tfm6406	3252
Turboprop	tp6410	3914

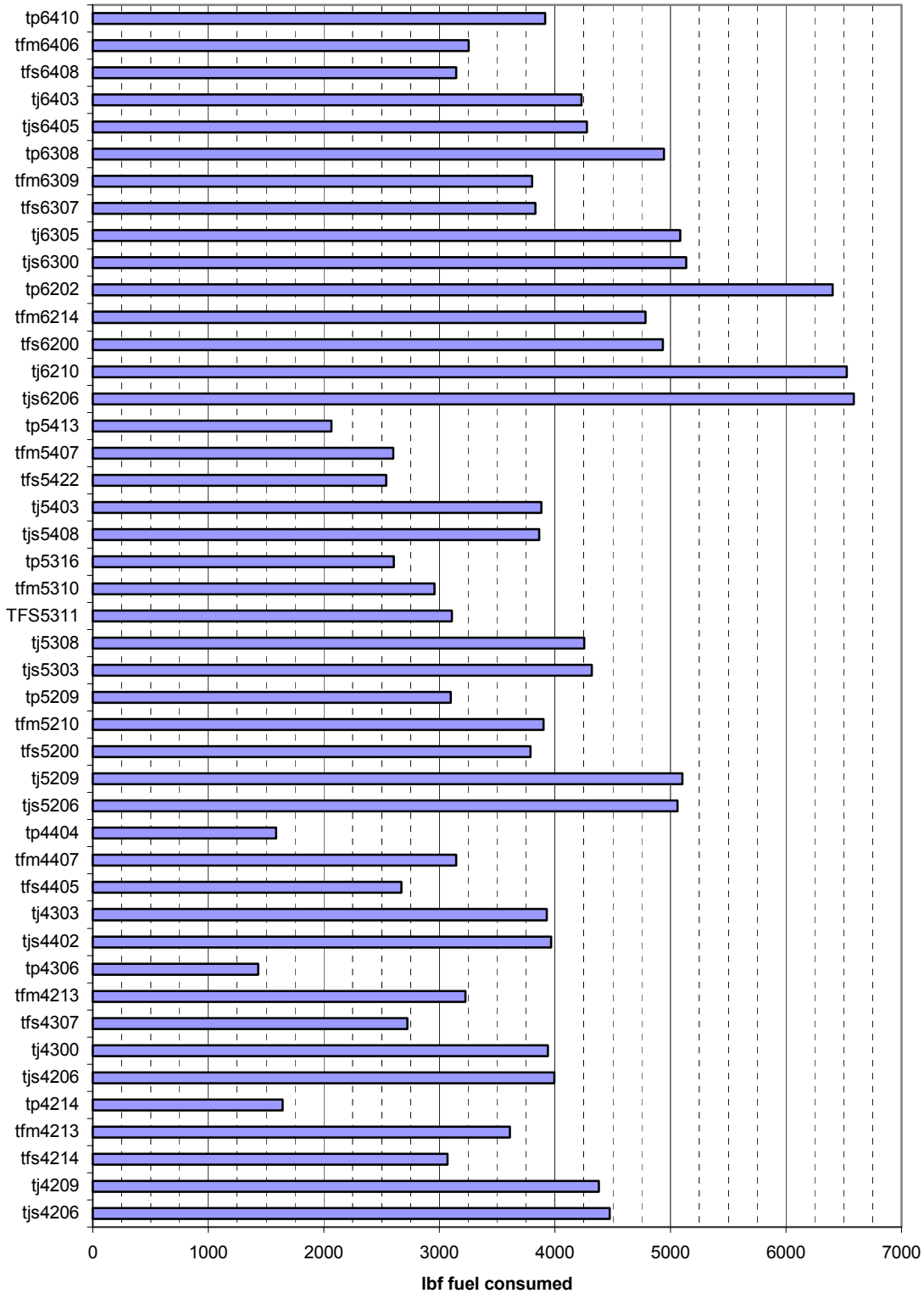

Fig. 8: Optimized Conventional engine Fuel Consumption Comparison

The first trend to consider was the effect of switchover Mach on fuel consumption. By comparing the engines in a Mach sweep across a specific switchover altitude, trends due to Mach number can be investigated.

At all switchover altitudes, the Mach 0.6 switchover case consumed the most fuel for all engine types and at all altitudes. Below is a sample figure of results (Fig. 9), comparing the total fuel consumed for the optimized engines at the 30 k ft switchover condition.

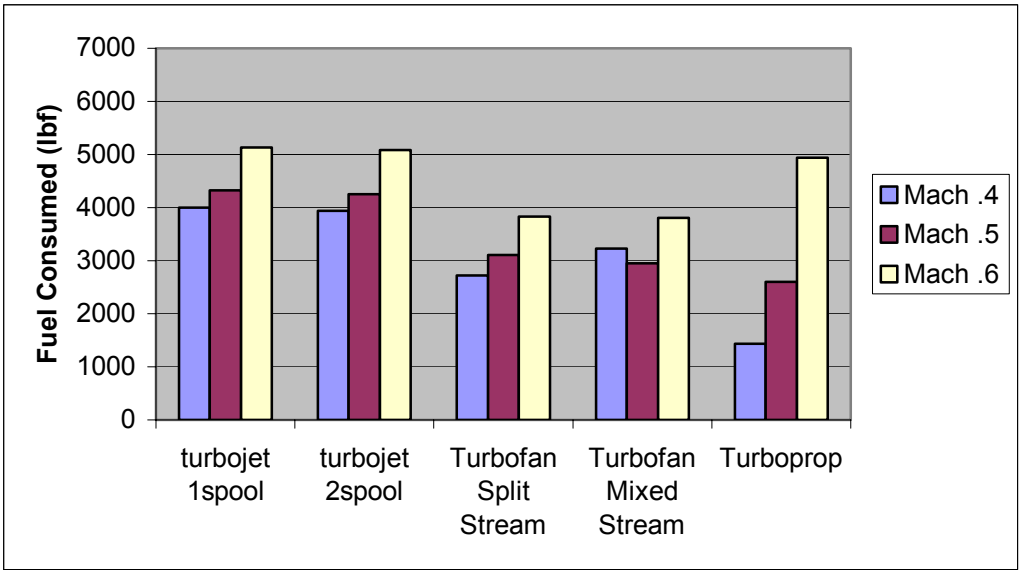

Fig. 9: Optimized Conventional engine fuel consumption comparison at 30,000 ft switchover altitude.

For the 20 and 30 k ft switchover cases, the most efficient switchover Mach number is 0.4, except for the mixed stream turbofan at 30 k ft. For the 40 k ft case, the optimum fuel efficiency is shown at Mach 0.5, with the exception of the turboprop that has the minimum fuel consumption at Mach 0.4. This effect of higher switchover Mach

number causing increased fuel consumption was expected due to higher drag associated with higher Mach numbers at similar altitudes.

Altitude sensitivity could be determined by examining altitude sweeps at a set Mach number. Altitude effects were more consistent than the Mach effects, with the trend pointing to the higher the switchover altitude, the less fuel consumed. This could be seen at each Mach number. Shown is an example result for comparing engines at Mach 0.5 (Fig. 10). The only exception to this rule was the Mach 0.4 turboprop engine where the 30 k ft was more efficient than the 40 k ft. Similar to the switchover Mach number effect, this altitude dependency was directly impacted by increased drag at lower altitudes.

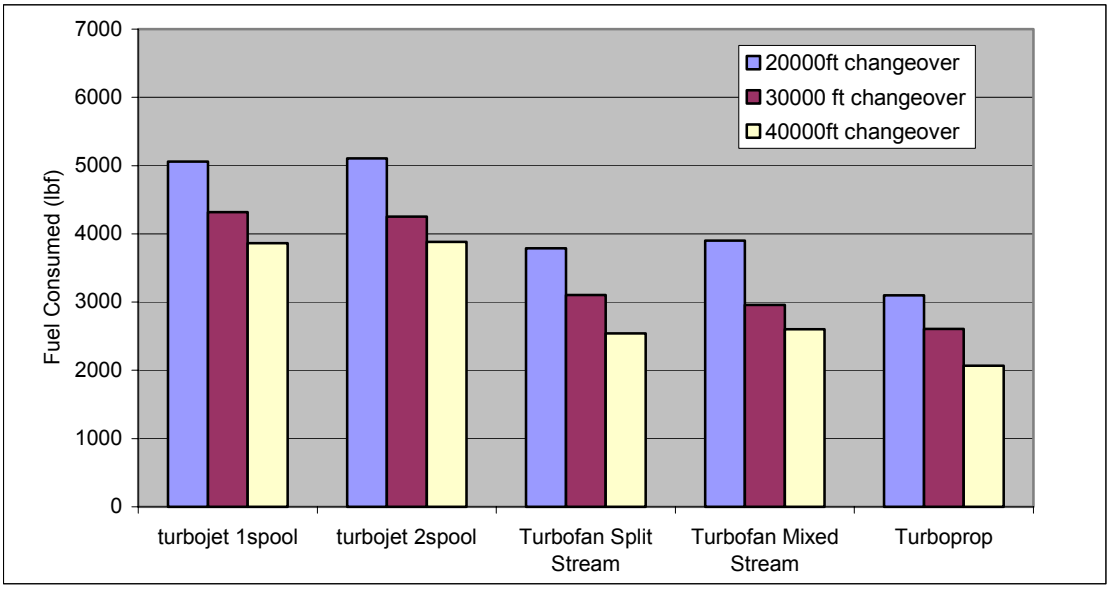

Fig. 10: Optimized Conventional engine fuel consumption comparison at Mach 0.5 switchover Mach

The final, but perhaps most important trend, is in the engine types themselves. In both Fig. 9 and Fig. 10 it can be seen that turbofans are more efficient than turbojets in any comparison. Turboprops are even better choices than turbofans except for switchover Mach numbers of 0.6. For the most part, differences between the single and dual spool turbojets are insignificant compared to the turbojet's difference from the other engine types. The same observation is made between the split stream and mixed stream turbofans. This engine type sensitivity falls in line with propulsive efficiency comparisons between engines (20: 29).

In review, the trends from the conventional engine optimization study show that a high switchover altitude and low switchover Mach number will result in the lowest fuel consumption regardless of engine type. The amount of fuel consumed during the conventional climb in every case was much smaller than the two 200-nmi switchover legs, thereby making the switchover condition the determining factor in fuel consumption. The turboprop consistently showed better fuel economy for all cases except the Mach 0.6 case. Since propellers lose propulsive efficiency at high mach numbers compared with turbofans, this is to be expected (27: 401). On the basis of fuel consumption alone the best engine across all switchover flight conditions is the turboprop, designated tp4306, flying the Mach 0.4, 30,000 ft switchover mission. AEDsys calculates engine tp4306 to consume 1,430 lbf (6.36 kN) of fuel during its entire notional conventional mission. By comparison, the worst selection using this method turned out to be the single spool turbojet, tjs6206, flying the Mach 0.6, 20,000 ft switchover mission; burning a total of 6585 lbs (29.3 kN) of fuel.

Note that even in the worst fuel consumption case, there is still approximately 8000 lbf (35.6 kN) saved in fuel. This means that if the TIHE components can be installed for less than 8000lbf, the modified HALE UAV would still have a takeoff weight of 25,600 lbf, while adding the increased endurance from the TIHE engine with no overall weight increase.

This leads to the conclusion that the conventional engine selection may not be as important to the feasibility of this aircraft as the TIHE engine selection will be. This allows for more flexibility of engine selection, if a hybrid engine is chosen.

4.3 TIHE Engine Selection Results

The first and most important result from running the optimized conventional engines through the TIHE missions in AEDsys, is that not all of the engines could provide adequate thrust at the higher altitudes. While the thrust requirements at the higher altitudes were significantly less than those at the lower altitudes, the optimization process used for the lower altitude flight caused poor performance at higher altitudes in some cases. The method used to get around this problem was to go back to the individual conventional optimization runs and attempt to run other engines, in the order of increasing fuel consumption, until an engine would work for the TIHE portion of the mission.

In all of the turbojet and turbofan cases, a suitable engine could be found from this method. None of the turboprops, however, could provide enough thrust at the cruise condition. In fact, many of the turboprops could not provide significant thrust above 40 k

ft. While it may be possible to design a turboprop engine to operate over the entire range of the mission, powered by both combustion and TIHE, it was deemed that for this study, the turboprop would be eliminated from consideration for the TIHE portion of the mission.

This left four engine types operating over the TIHE mission legs at all of the switchover conditions. The required power values were calculated at several of the climb flight conditions and the maximum, minimum, and cruise required power values were tabulated. These values are listed in Table 4 and shown in Fig. 11, with additional information listed in Appendix B.

Table 4: Max, Min, and Cruise Required Power for TIHE engine Selection

Engine #	Engine Type	Max Power (MW)	Min Power (MW)	Cruise Power (MW)
Mach 0.4				
tjs4206	Single Spool Turbojet	8.244	3.756	3.756
tj4209	Dual Spool Turbojet	8.077	3.867	3.873
tfs4213	Split Stream Turbofan	5.916	2.987	3.051
tfm4213	Mixed Stream Turbofan	6.244	2.748	2.748
tjs4206	Single Spool Turbojet	5.228	3.776	3.795
tj4300	Dual Spool Turbojet	5.187	3.866	3.916
tfs4307	Split Stream Turbofan	3.579	2.798	2.896
tfm4213	Mixed Stream Turbofan	4.035	2.761	2.761
tjs4402	Single Spool Turbojet	3.916	3.672	3.807
tj4303	Dual Spool Turbojet	4.033	3.712	3.935
tfs4403	Split Stream Turbofan	2.976	2.565	2.924
tfm4403	Mixed Stream Turbofan	2.888	2.75	2.775
tfm5407	Mixed Stream Turbofan	2.65	2.493	2.567
Mach 0.5				
tjs5203	Single Spool Turbojet	13.38	3.856	3.856
tj5208	Dual Spool Turbojet	13.62	3.888	3.888
tfs5200	Split Stream Turbofan	9.811	3.057	3.057
tfm5200	Mixed Stream Turbofan	9.25	2.588	2.588
tjs5303	Single Spool Turbojet	8.358	3.757	3.757
tj5308	Dual Spool Turbojet	8.303	3.898	3.898
tfs5303	Split Stream Turbofan	6.18	3.093	3.093
tfm5309	Mixed Stream Turbofan	5.871	2.843	2.843
tjs5408	Single Spool Turbojet	5.096	3.745	3.745
tj5403	Dual Spool Turbojet	5.16	3.922	3.922
tfs5403	Split Stream Turbofan	3.818	3.006	3.023
tfm5407	Mixed Stream Turbofan	3.42	2.567	2.567
Mach 0.6				
tjs6206	Single Spool Turbojet	23.29	3.604	3.604
tj6210	Dual Spool Turbojet	23.3	3.774	3.774
tfs6203	Split Stream Turbofan	17.82	3.039	3.039
tfm6211	Mixed Stream Turbofan	15.31	2.631	2.631
tjs6300	Single Spool Turbojet	14.17	3.668	3.668
tj6305	Dual Spool Turbojet	14.23	3.814	3.814
tfs6310	Split Stream Turbofan	10.84	3.062	3.062
tfm6305	Mixed Stream Turbofan	9.418	2.657	2.657
tjs6405	Single Spool Turbojet	8.423	3.743	3.743
tj6403	Dual Spool Turbojet	8.453	3.862	3.862
tfs6408	Split Stream Turbofan	6.316	2.988	2.988
tfm6401	Mixed Stream Turbofan	5.687	2.675	2.675

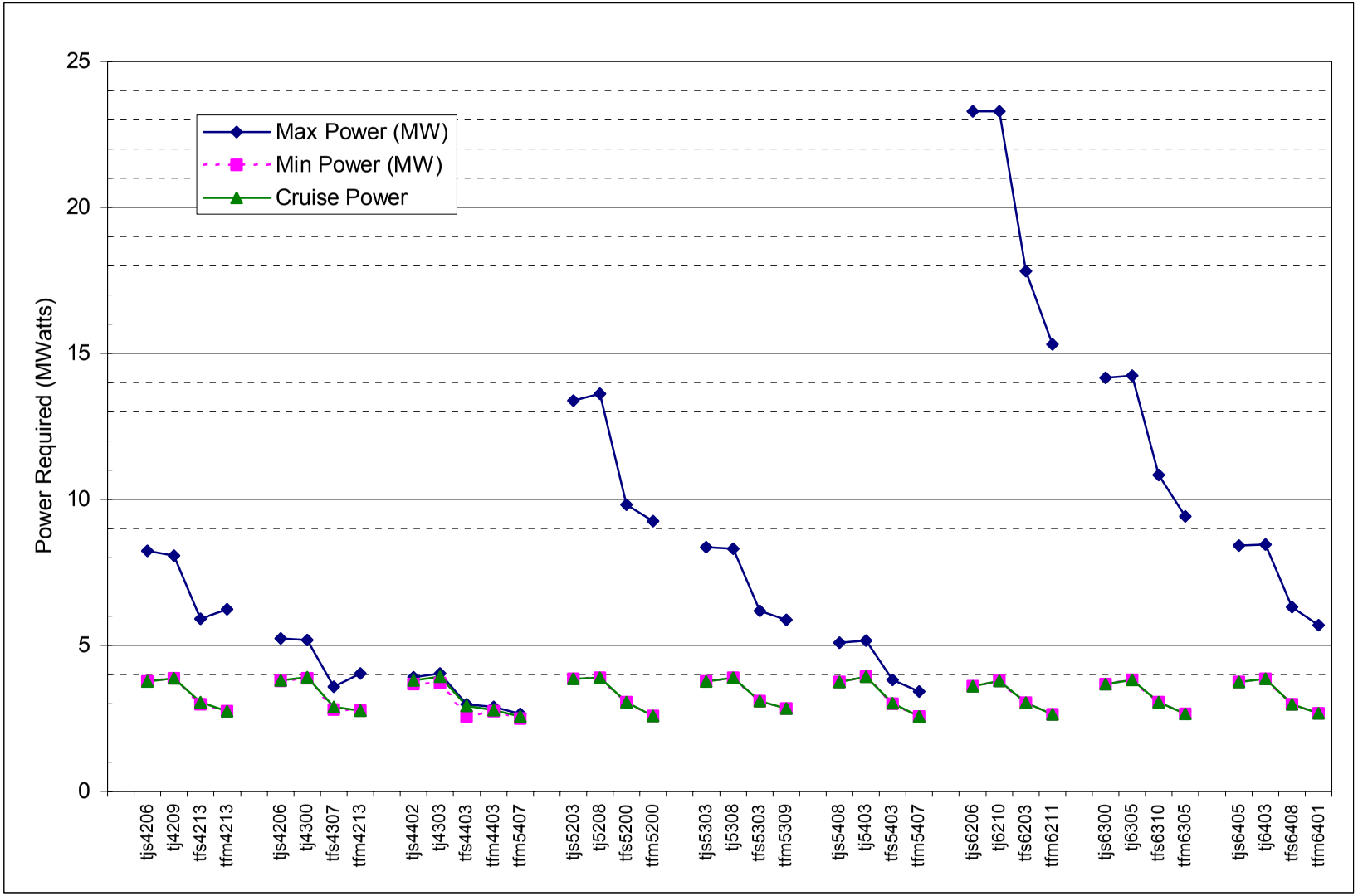

Fig. 11: Maximum, Minimum, and Cruise Required power for TIHE engine selection

The trends in each of these values were evaluated to aid in choosing the best selection for TIHE engine. The most important value with respect to weight was maximum required power.

As the conventional engines showed, several trends became evident in reducing the maximum required power by the TIHE. By examining a set switchover altitude along with a switchover Mach sweep, maximum required power throughout the climb is lowest at the lower Mach number. This can be seen clearly in a look at the 30 k ft switchover comparison of maximum required power (Fig. 12). This trend of the Mach 0.4 switchover condition, needing the lowest maximum power, is repeated across the other two switchover altitudes. This result is due to lower drag at lower Mach numbers for the same altitude.

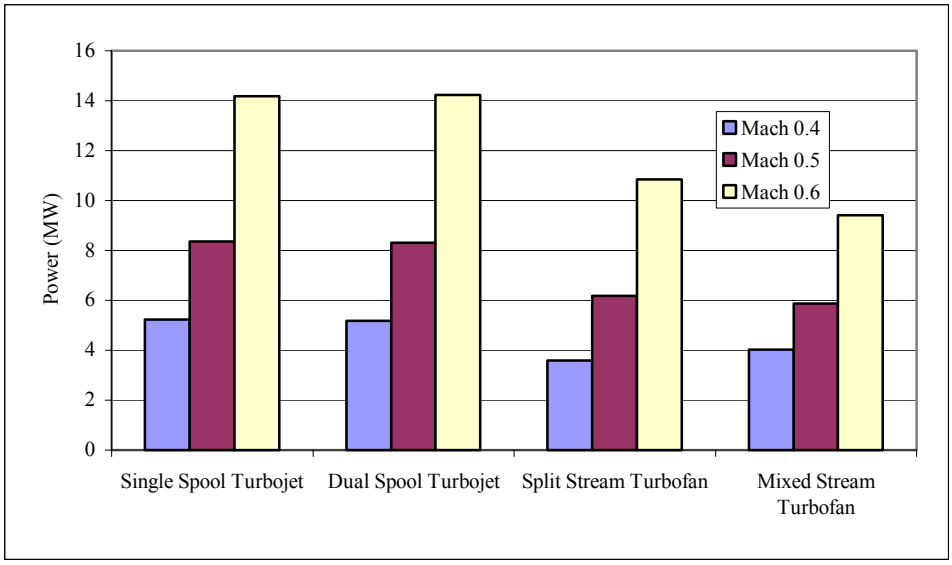

Fig. 12: TIHE engine max required power comparison at the 30 k ft switchover altitude

Locking the switchover Mach and comparing switchover altitudes demonstrates the importance of switchover altitude in reducing maximum power. The 40 k switchover altitude allowed for the smallest maximum required power out of all of the altitude comparisons. Fig. 13 shows the comparison of Max required power for engines at different switchover altitudes at Mach 0.5 switchover condition. The higher altitude for switchover results in lower maximum required power, due to lower drag.

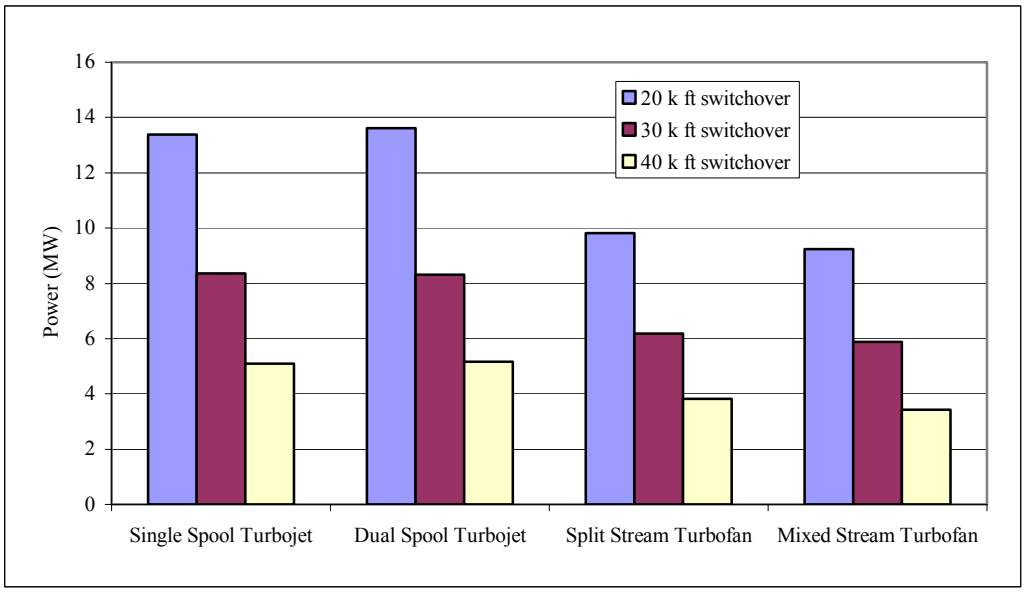

Fig. 13: TIHE Engine Max Required power Comparison at Switchover Mach of 0.5

By comparing all of the maximum required power values for all engine types, both of the turbofans had consistently lower numbers than the turbojet types. This points to the turbofan as a better choice as the TIHE powered engine. The engine and switchover combination that produced the lowest max required power was the tfm4403 at switchover conditions of Mach 0.4 and 40,000 ft altitude. This engine required only 2.89

MW of power at its highest power consumption level. The split stream turbofan (tfs 4403) with the same switchover conditions was a close second with a maximum power requirement of 2.98 MW.

While this comparison showed that maximum required power was highly sensitive to switchover conditions, another value was needed to compare all of the engines at the same operating conditions. Since all of the engines were run at Mach 0.6 and 60,000 ft, and a best cruise altitude condition for Mach 0.6, these values could be used to compare engines regardless of the switchover conditions. This would find the best engine for the main cruise and loiter phases that make up the majority of the entire mission.

These cruise power requirements are co-located with the maximum required power numbers from the TIHE AEDsys runs in Table 4. Only about 2 MW differentiated the best engine from the worst, however again the turbofans performed better than the turbojets with regard to the cruise power. The best cruise performance of any engine was the mixed stream turbofan chosen for the Mach 0.5, 40,000 ft switchover, the tfm5407, with a cruise power value of 2.57 MW.

Since cruise performance for this engine was better than the engines chosen due to lowest maximum power, it was decided to run engine tfm5407 at the Mach 0.4, 40,000 ft switchover TIHE mission. This would enable direct comparisons of the two best engines chosen for the different criteria to be compared in all of the same criteria.

When the tfm5407 engine was run, the maximum required power was 2.65 MW. This value was smaller than the tfm4403 by 0.24 MW. This leads to the selection of the tfm5407 engine as the most efficient choice for the TIHE engine configuration, while

choosing the Mach 0.4, 40,000 ft switchover as the most efficient to keep maximum power requirements, for any engine, low.

4.4 Shielding Sensitivities

While shielding issues were addressed in Chapter 3, there were several issues to be examined further and were included in the research to ensure completeness. Assumptions about equipment tolerance, distance from source to sensitive equipment and the amount of radiation as a percent of total power produced were tested for sensitivity of shielding weight amounts. The same equations (eqns. 16-20) developed in Chapter 3 were utilized for this portion of the study and the assumed values were used as the baseline case. The semi-spherical shield was utilized for these results.

Studied first was the sensitivity of equipment tolerance to radiation on shielding weight. Values on equipment tolerances ranged from 10^{-6} to 1 rad/sec and the results can be seen in Fig. 14. While equipment tolerances do affect shield weight significantly, it shows a directly logarithmic relationship and even for human tolerance levels of 10^{-6} rad/sec, the shield weight does not become prohibitive.

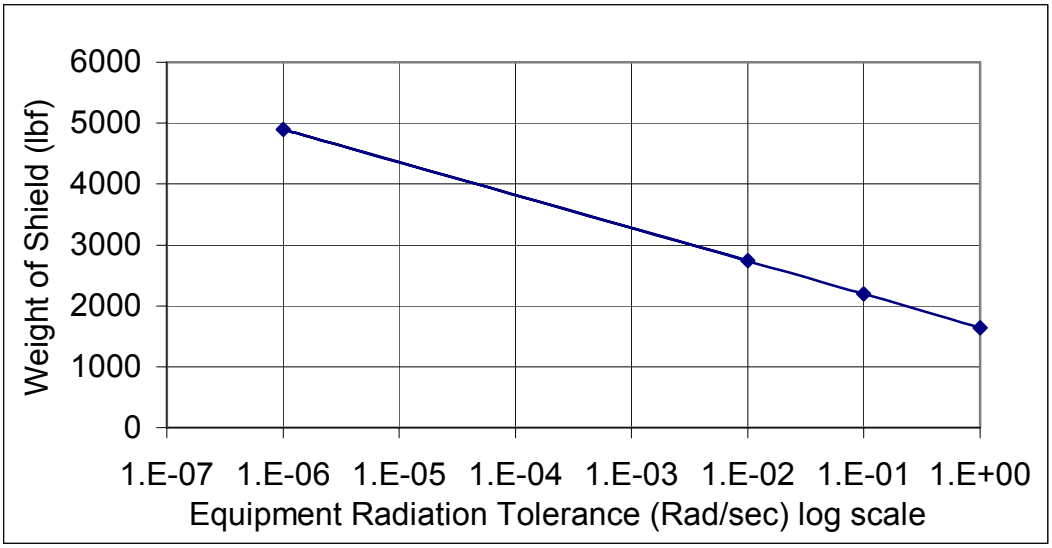

Fig. 14: Shield Weight Sensitivities to Equipment Radiation Tolerances

The sensitivity of equipment distance from the source on shielding weights was studied next. Distances ranged from 0.5 m, to represent equipment as close as engine control units, located within the engine cowling, to 5.0m, representing the most sensitive ISR equipment located in the far forward compartment of the HALE UAV. The results are shown in Fig. 15. With all other parameters staying the same, there is only a 1,200 lbf (5.34 kN) difference in shielding requirements if the most sensitive equipment is in the engine cowling compared with the front sensor section. This allows us to continue to utilize our 3 m assumption for our working model.

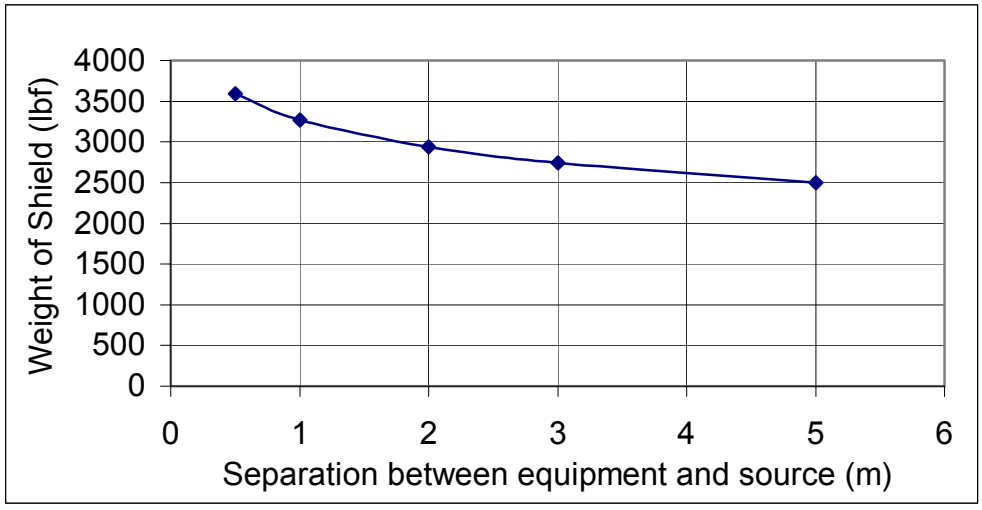

Fig. 15: Shield Weight Sensitivities to Equipment-Source Separation

The final sensitivity study accomplished for the shielding results was to test the assumption of needing to shield only 5% of the total power produced by the TI source as radiation. How would the shield weight be changed if a higher percentage of radiation leaked and needed to be shielded? A range of 5% to 90% was tested and the results are shown in Fig. 16. There turned out to be only a difference in shield weight of around 700 lbf (3.11 kN). This is due to the logarithmic nature of equation 18. This means that even if the TI source is very leaky, the shielding weights will not have to be significantly increased.

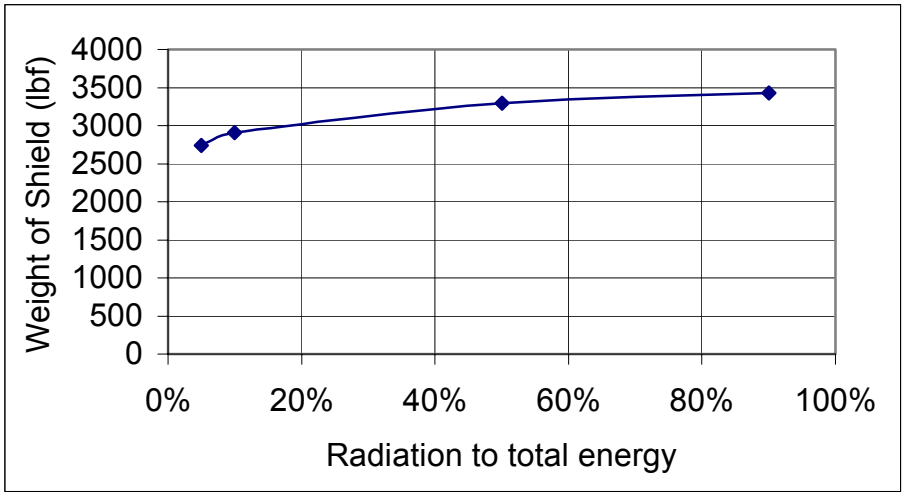

Fig. 16: Shield Weight Sensitivities to Radiation Percentages

Results from this sensitivity study show that even if some of the assumed values are incorrect, the shielding weight will still be on the order of the values calculated by this study.

4.5 Selection of Hybrid Engine

With the results from both the conventional engine and the TIHE engine optimization runs, several decisions regarding a selection of engine or engines were made. While the possibility of two separate engines, one based on combustion and the other on a TIHE powered engine, remains; trends within both studies point to a single hybrid engine as the best selection for the HALE UAV mission proposed.

Turboprops in the Mach 0.4 switchover cases were better in fuel consumption by around 1000 lbf compared to the best engine of any other type. However, the degraded performance of turboprops at the higher altitude and higher Mach numbers kept them

from being considered for use as a TIHE powered engine. At this point, the option of having a turboprop as the conventional engine and a turbofan as the TIHE engine had to be examined. The issues of added engine weight of the second engine, of dealing with non-operating propellers during the TIHE portion of the mission, and added modification and maintenance requirements, made the two-engine model unappealing.

As a counterproposal to the two engine model, the results of both the conventional and TIHE engine selections point to the fact that a mixed stream turbofan engine could fly the entire mission with a switchover flight condition of Mach 0.4 and 40,000 ft and be the most efficient of all of the turbojets and turbofans tested. In Fig. 17, all of the important parameters (fuel consumed, max power, and cruise power) converge on the tfm5407 as the best engine to be used as a hybrid.

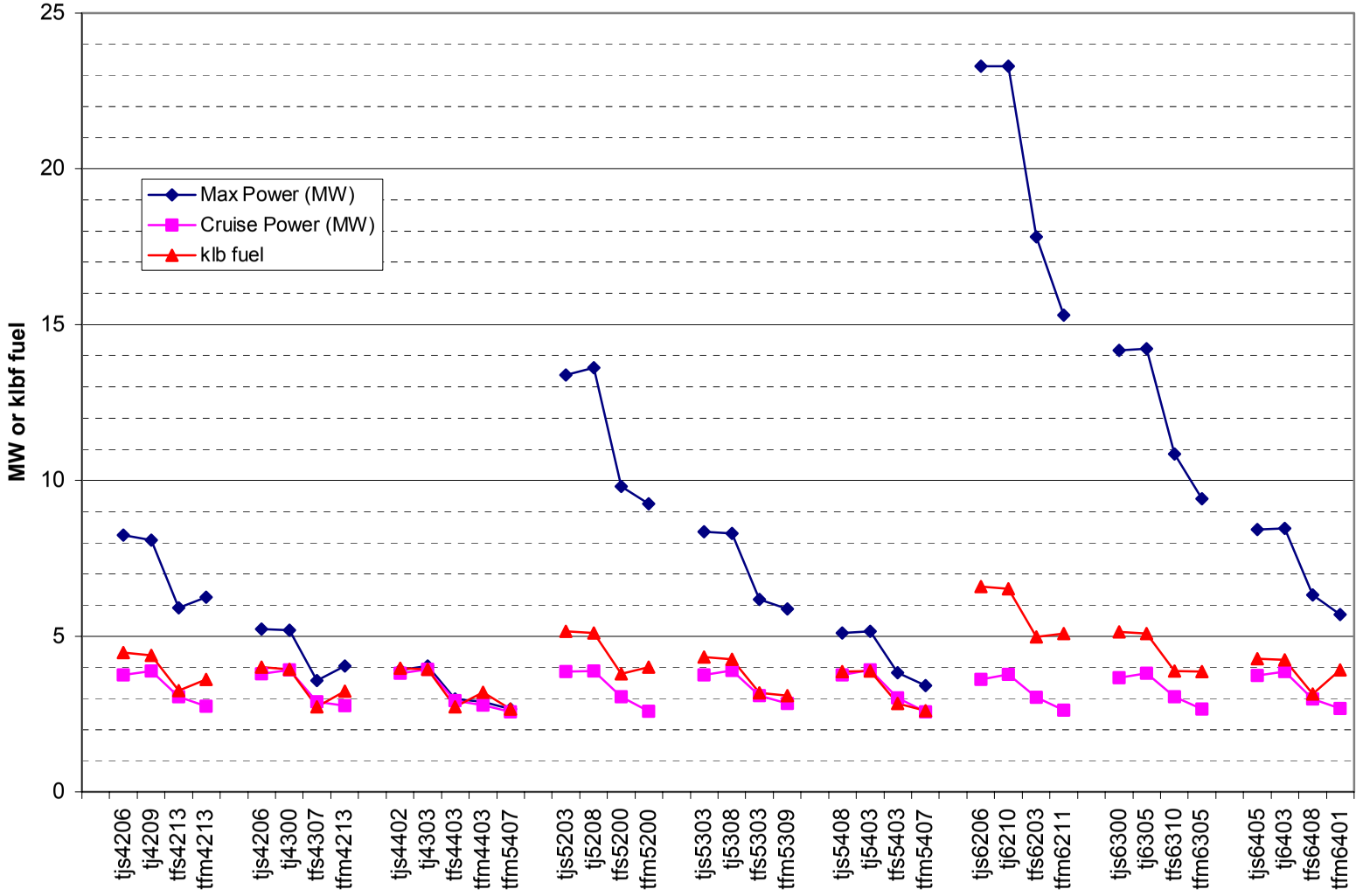

Fig. 17: Fuel Consumed, Max, and Cruise Required Power comparisons for TIHE optimized engines

In Table 5, the design parameters that created the tfm5407 are listed.

Table 5: TFM5407 Turbofan Engine design paramaters

On-Design	
Mach	0.5
Altitude	25,000 ft
π_C	30
LPC π	2.4
Fan π	2.4
Bypass Ratio α	4.1
Max T_{T4}	3200° R
Engine Size	
Inlet Area	6.38 ft^2
Exit Nozzle Area	3.50 ft^2
Nozzle Length	3.80 ft

This hybrid combustion-heat exchanger engine concept had been examined as a possible choice for the nuclear fission powered jet engines of the US and USSR's atomic aircraft programs (1, 2, 11, 14). Since this choice also eliminates the need for a second engine and all of the structural and maintenance issues associated with a second engine, the addition of the 1000 lbf (4.45 kN) of extra fuel needed by the turbofan was deemed favorable.

4.6 Modified Aircraft Weight Calculations

With the selection of the mixed stream turbofan, tfm5407, as the best choice as a hybrid engine, aircraft component weight calculations could be made. Since the initial optimization and engine selection process was complete, the engine, tfm5407, selected for the hybrid engine configuration was redesignated TIHEX1 for the remainder of the study. The weight values listed here should be considered conservative approximations, because care was taken not to underestimate weights. The weights calculated here fall into three categories: current configuration hardware, new fuel weights, and TIHE component weights.

With the assumption that minimal structural changes would be made to the airframe, the airframe weight stays the same. The engine weight for the conventional sections of the TIHEX1 engine will be assumed to be roughly the same as the AE3007 turbofan engine on board the current configuration of the Global Hawk. Any additional weight from the TIHE portion will be accounted in the TIHE component weights. While the decrease in fuel weight allows for additional payload to be added, this value was also kept at its current weight.

The assumption that the aircraft would takeoff at the 25,600 lbf (113.9 kN) weight was again used to begin calculations. A new mission was inputted into AEDsys: consisting of the entire conventional-TIHE mission with the Mach 0.4, 40,000 ft switchover point. Fuel weights were the calculated fuel consumed value of 2,616lbf (11.6 kN) and a 25% contingency fuel reserve of 654 lbf (2.9 kN). This represents a 77% drop in fuel weight from the current HALE UAV configuration.

Also from this AEDsys run, maximum required power for the TIHE mission was calculated for the correct weight of the aircraft, at that point in the mission. That value of 2.897 MW was then used in the calculation of shielding weights following the method described in chapter 3. The weight of a semispherical shield placed a distance of .5 m from the source was 2,616 lbf (11.6 kN).

A weight estimate for the heat exchanger itself was selected from Hartsfield's heat exchanger research and modified to include a safety factor of approximately 20% (6: 4-16). The weight used was 1,500 lbf (6.67 kN) and represents the conservative case for heat exchanger weights. The required TIHE fuel weight was added to ensure completeness, but did not amount to a significant percentage of the total weight.

Additional weight needed to be included in this study for the X-ray triggering device and additional modifications made to the engine to allow switchover. Since operational devices have not been manufactured yet, a very rough estimate needed to be made. Several methods were considered ranging from a required power correlation method to a fixed weight. In the end, a fixed weight of 2000 lbf (8.9 kN) was chosen for simplicity.

With all of the weights accounted for, a value for the eliminated weight was easily calculated. A 5,012 lbf (22.3 kN) or 20% decrease in weight of the HALE UAV was possible using a hybrid conventional-TIHE turbofan engine for its mission. This value again represents only a conservative first run iteration on engine selection. A breakdown of component weights by percentage is shown in Figure 18. This breakdown represents a 7-day TIHE cruise and loiter phase with engine switchover at 40,000 ft and Mach 0.4.

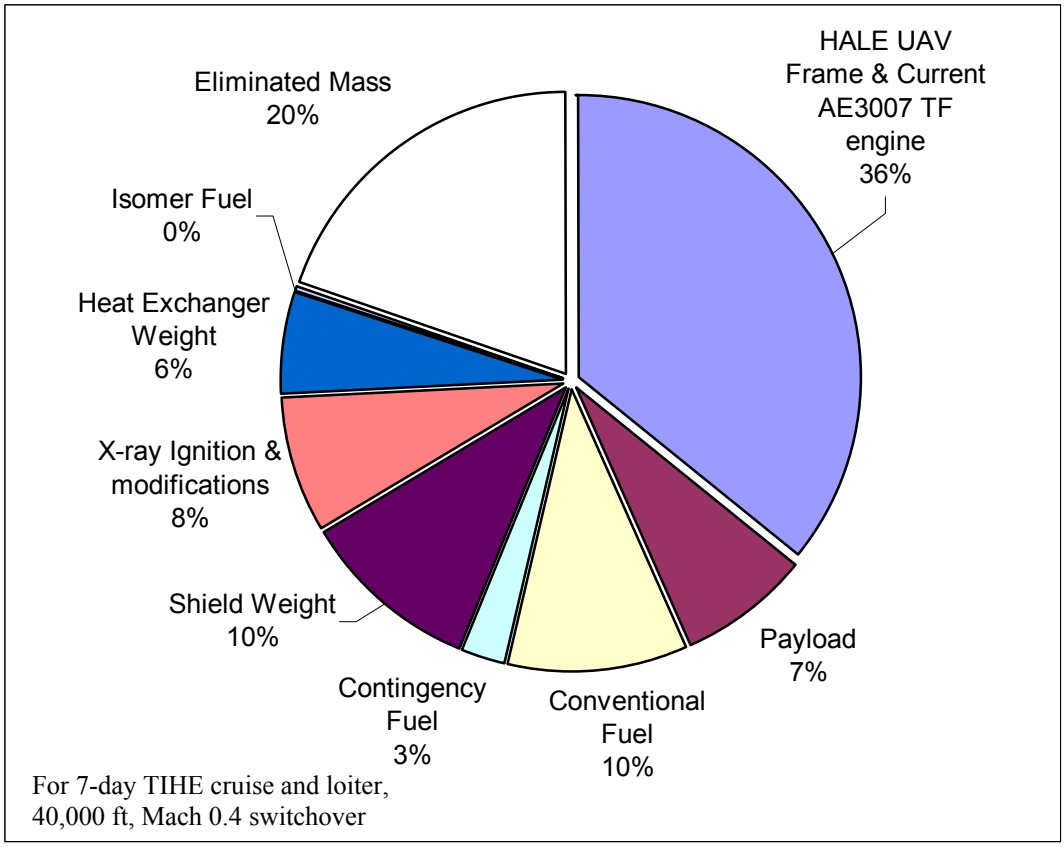

Figure 18: Weight Breakdown by Percentage of Hybrid powered Turbofan

If 20% of the weight was eliminated prior to takeoff, the propulsion requirements decrease significantly, requiring a smaller engine, burning less fuel for the conventional portion. In the same manner, power requirements for the TIHE portion of the mission will also drop, culminating in smaller shield weights. These factors will quickly lead to an even larger decrease in takeoff weight.

An iterative method based on this concept was carried out in a second run to investigate how much more the weight could be reduced. The results are tabulated along with the results from the first weight values in Table 6. Several AEDsys programming

issues required a slight modification of the sea level loiter phase for the second run, however final fuel consumed values fell in line with expectations.

Table 6: Weight Calculations for Hybrid powered Global Hawk

Components	TIHEX1	TIHEX2
Take off Weight	**25600**	**20586**
Current Configuration		
Global Hawk Frame & Current AE3007 TF engine	9200	9200
Payload	1900	1900
Dry Weight	**11100**	**11100**
Fuel		
Conventional Fuel	2616	2371
Contingency Fuel	654	593
Fuel Weight	**3270**	**2964**
TIHE Components		
Shield Weight	2616	2577
X-ray Ignition & modifications	2000	2000
Heat Exchanger Weight	1500	1500
Isomer Fuel	100	100
TIHE Weight	**6216**	**6177**
Eliminated Mass	**5014**	**346**
New TO weight	**20586**	**20240**

*All weights are in lbf

The second iteration started with a takeoff weight of 20,586 lbf (91.6 kN) and resulted in only a small decrease in shield and fuel weight, compared to the first iteration.

A drop of approximately 346 lbf shows that the iterative process converges quickly on a weight breakdown.

4.7 Additional Results

In order to compare performance of this turbofan hybrid engine, with the J-57 engine studied by Hartsfield (6), heat required power calculations were also made along the conventional legs. These values only represent the max power needed during each leg. It is important to note, that these calculations assume the TIHE is providing momentary thrust and takes into account the decreasing weight of the aircraft due to fuel consumption.

Results, from both iterations of the hybrid TIHEX engines, determined that the maximum required power during the entire flight was 17.5 MW at sea level static conditions. This represents around 40% of the required power to drive the J-57 engine at full thrust as shown in Hartsfield's work (6). The lower power requirements are due to lower thrust values and better engine efficiencies. Shield requirements calculated for this full TIHE power version shows the weight of 3,043 lbf (13.5 kN) or an increase of only 16%. If the entire mission was flown with the TIHE engine and the conventional fuel was eliminated an additional 2,800 lbf (12.5 kN) could be eliminated from the weight.

5. Conclusions and Recommendations

This chapter summarizes the research conducted and contains conclusions based on the current research and recommendations for continued research.

5.1 Summary of Research

This study consisted of a selection of a High Altitude Long Endurance ISR platform as the best application of TIHE power to jet engines. Due to radiation and life support concerns, using a UAV for this mission was deemed appropriate and the Global Hawk vehicle was selected as a baseline HALE UAV for this study. Selection of switchover Mach and altitude conditions were made in conjunction with engine type in two separate processes, conventional and TIHE powered flight. The use of engine design (ONX) and mission analysis (AEDsys) software allowed for optimization of engine types for each of the nine different switchover conditions. The optimization for the conventional engine hinged on lowest fuel consumption, while the TIHE optimization was based on maximum and cruise required power. Additionally, radiation shield weight was calculated based on TIHE maximum required power. The calculated weights of airframe, chemical fuel, heat exchanger, triggering mechanism, and radiation shield led to weight comparisons to the Global Hawk reference vehicle.

5.2 Conclusions

The following conclusions are shown here based on the work done during this study.

1. A turbofan is the best choice for a hybrid chemical-TIHE jet engine for use as the primary propulsion unit of a HALE ISR UAV. It is the most efficient engine in its cruise condition at high altitudes, where the aircraft will spend most of its mission. The turbofan also provides sufficient thrust at a reasonable fuel consumption rate during low altitude flight.

2. Shielding requirements, that hindered the fission powered aircraft program, are significantly reduced due to the lack of neutron and radioactive product release in a triggered isomer reaction. This reduction in radiation results in tremendous drops in shield weight. Also, the use of the TI source in unmanned vehicles reduces the shield weight appreciably.

3. The use of the hybrid turbofan powered by the TIHE for the cruise and loiter legs of the mission will not only provide almost limitless endurance but will also drastically decrease the weight of a conventional HALE UAV by 20% or more.

4. If the restrictions on running the TI source at takeoff were removed, the TIHE is capable of providing the heat power for the entire mission, with only a slight increase in shielding weight required. The decrease or elimination of fuel and associated systems would net an even larger decrease in total weight.

5. Engine configuration could be as simple as an inline direct cycle heat exchanger followed by the combustor. This configuration has been successfully tested in

the HTRE tests (14) and could allow the controlled start up of the TIHE while still providing thrust for flight. While the ability for a TIHE to power the turbofan engine does not rely specifically on the engine configuration, this in-line direct cycle shows promise.

5.3 Recommendations

The results from this research, point in several interesting directions for future study. They are listed here in no particular order of importance.

1. A more intensive optimization of a turbofan engine for hybrid use could be accomplished with the reduced weight values. This study was limited into broad selection criteria ending with the selection of engine type. The goals of this research did not require a more rigorous optimization study. It is possible that with such an optimized engine, fuel and power requirements would be even lower, again reducing the weight of the aircraft.

2. Utilizing the heating requirements found in this study, the design of the actual heat exchanger to be used for this engine could be accomplished using methods similar to Hartsfield's research. An examination of both a direct and in-direct cycle could be examined as was done during the NEPA/ANP programs.

3. Research into the configuration of the engines, shielding, and ignition system would also benefit the research previously accomplished. Again, significant work has been accomplished in this arena during the design of fission powered aircraft.

4. While this study focused on the HALE UAV application, other applications could be studied. Missions such as Air Launched Cruise Missiles would have many similarities to this study, but the need for conventional propulsion might be eliminated due to the air launch. Rockets, powered by TI reactions, also hold great promise for spacelift and interplanetary propulsion.

References

1. Perel'Man, R. G. *Soviet Nuclear Propulsion (Yadernyye Dviagateli)*. Washington, D.C.: Triumph Publishing Co., 1959.

2. Keirn, Donald J. "The USAF Nuclear Propulsion Programs" in *Nuclear Flight: The United States Air Force Programs for Atomic Jets, Missiles, and Rockets*. Ed. Kenneth F Gantz. New York: Duell, Sloan, and Pearce, 1960.

3. Megazone. "The Decay of the Atomic Powered Aircraft Program," Undergraduate Research Paper from Worcester Polytechnic Institute, Worcester, MA, 1993.

4. Collins, C.B., F. Davanloo, M.C. Iosif, R. Dussart, J.M. Hicks, S.A. Karamian, C.A. Ur, I.I. Popescu, V.I. Kirischuk, J.J. Carroll, H.E. Roberts, P. McDaniel, and C.E. Crist. "Accelerated Emission of Gamma Rays from the 31-yr Isomer of 178Hf Induced by X-Ray Irradiation," *Physical Review Letters*, 82-695-698 (January 1999).

5. McDaniel, Pat. "Triggered Isomer Research Program: Propulsion Aspects." Memorandum from AFRL/DEPA, undated.

6. Hartsfield, C. R., "Analysis of the Application of a Triggered Isomer Heat Exchanger as a Replacement for the Combustion Chamber in an Off-the-Shelf Turbojet." MS Thesis, AFIT/GAE/ENY/01M-04. School of Engineering and Management, Air Force Institute of Technology (AU), Wright-Patterson AFB OH, March 2001.

7. Air Combat Command. "RQ-4 Global Hawk Unmanned Aerial Vehicle" Fact Sheet. Langley AFB, VA. 2000.

8. Glover, Eugene. "Air Combat Command Concept of Operation for the Global Hawk Unmanned Aerial Vehicle Draft Version 2.0." Langley AFB, VA. August 2000.

9. Northrop-Grumman. "Global Hawk Air Vehicle Outline" Data Sheet. Ryan Aeronautical Center, August12, 1999.

10. Rolls-Royce "Rolls-Royce: Civil Aerospace-AE3007" Product fact sheet. n. pag. http://www.rollsroyce.com/civil/products/turbofans/ae3007/detail.htm. June 12, 2001

11. Subcommittee on Research and Development of the Joint Committee on Atomic Energy. *First Session on the Aircraft Nuclear Propulsion Program*. Hearing, 86th Congress, 1st Session, July 28, 1959. Washington: GPO, 1959.

12. Miller, Jay. *The X-Planes*. Arlington, TX: Aerofax, Inc, 1988.

13. Cleveland, F.A. and Johnson, Clarence L., "Design of Air Frames for Nuclear Power", *Aeronautical Engineering Review,* 16:pg 48-57, June 1957.

14. Shoults, D. R. "Direct-Cycle Nuclear Propulsion." in *Nuclear Flight: The United States Air Force Programs for Atomic Jets, Missiles, and Rockets*. Ed. Kenneth F Gantz. New York: Duell, Sloan, and Pearce, 1960.

15. Jones, R.I. "The design challenge of high altitude long endurance (Hale) unmanned aircraft." *The Aeronautical Journal*, pp. 273-280, June 1999.

16. "Global Hawk Program Data" Global Hawk Program office ASC/RAV, Wright-Patterson AFB, OH. August 2001.

17. Mattingly, Jack D., Heiser, William H., Daley, Daniel H. *Aircraft Engine Design*. New York: American Institute of Aeronautics and Astronautics, Inc., 1987.

18. Mattingly, Jack. AEDSYS: Aircraft Engine Design System Analysis Software (Version 2.13 – December 14, 2001 for Windows 95/98/NT). From website http://www.aircraftenginedesign.com with permission of author.

19. Mattingly, Jack. ONX: Parametric Cycle Analysis –On Design Analysis of Gas Turbine Engines. (Version 4.021- December 18, 2001 for Windows 95/98/NT.) From website http://www.aircraftenginedesign.com with permission of author.

20. Mattingly, Jack. *Elements of Gas Turbine Propulsion*. New York: McGraw-Hill, Inc., 1996.

21. Bruening, Gary. "Future Propulsion Capability – Sensorcraft" unpublished presentation. Air Force Research Laboratory, AFRL/PRTA, Wright-Patterson AFB, OH.

22. Propulsion Product Group Manager, *The Engine Handbook*. San Antonio Air Logistics Center, TX. March, 1998.

23. Automation Creations, Inc. "MatWeb: The online Materials Information Reference." Reference web page. n. pag. www.matweb.com. December 18, 2001.

24. Turner, James E. *Atoms, Radiation, and Radiation Protection* (Second Edition). New York: John Wiley & Sons, Inc., 1995.

25. Carson, M., Diz, R., Long, S., MacArthur, K., Totty, K. Radiation Hardening in Space, "Radiation Hardening of Electronics." MSE 4206 Class Presentation, Virginia Tech, VA. Web site. http://www.mse.vt.edu/faculty/hendricks/mse4206/projects97/group02/space.htm#summary. December 1997.

26. Wetch, Joseph R. "Nuclear Reactors as Auxiliary Power Sources" in *Nuclear Flight: The United States Air Force Programs for Atomic Jets, Missiles, and Rockets*. Ed. Kenneth F Gantz. New York: Duell, Sloan, and Pearce, 1960.

27. Raymer, Daniel P. *Aircraft Design: A Conceptual Approach.* Reston, VA: AIAA, 1999. pp 401.

Appendix A: Conventional Engine Selection Data and Graphs

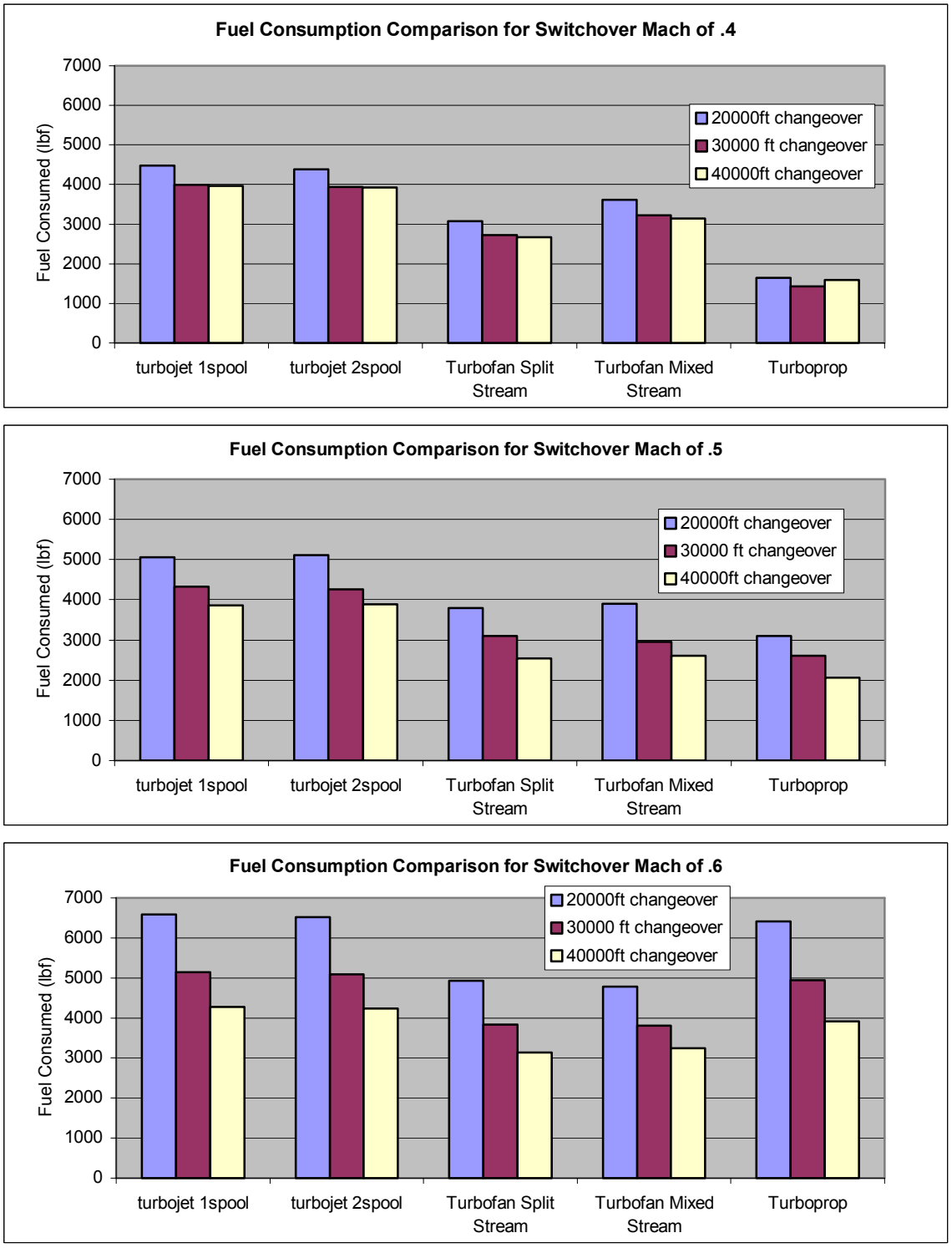

Optimized Conventional Engines: Comparison at specific Mach number with altitude Sweep

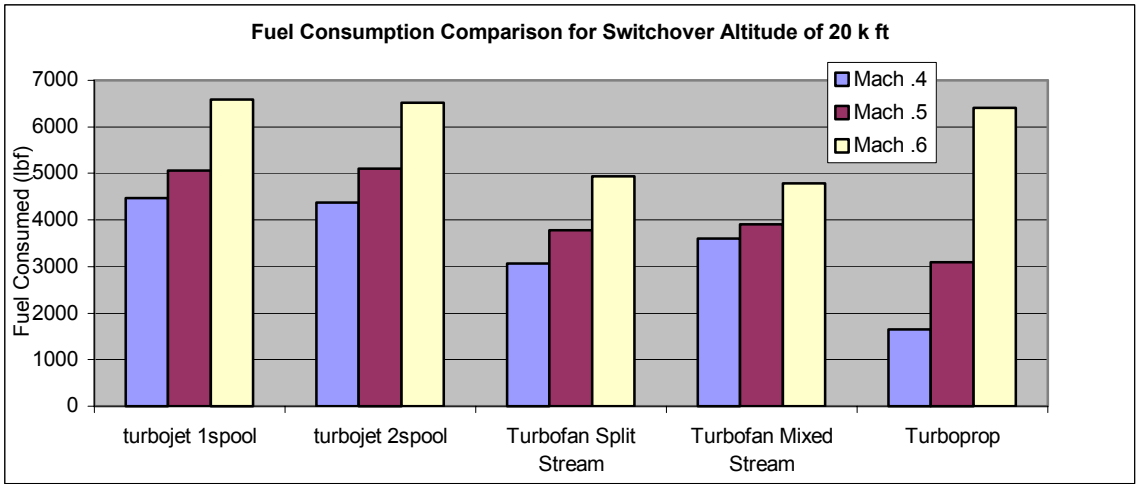

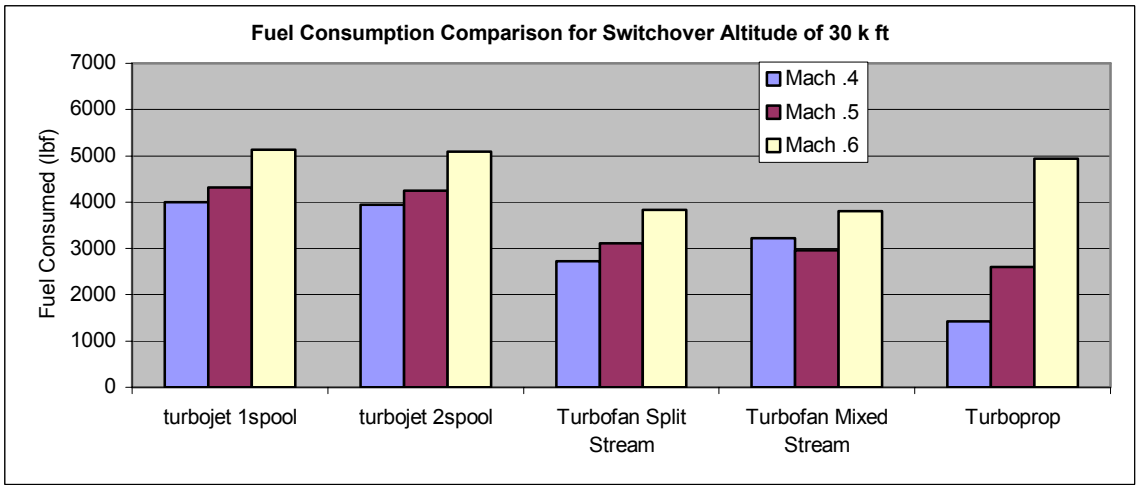

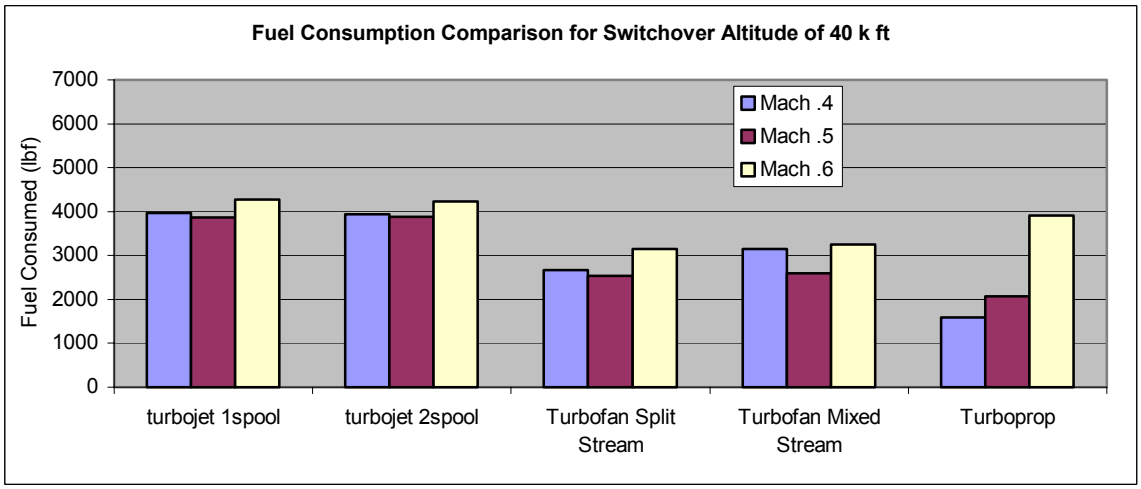

Optimized Conventional Engines: Comparison at specific altitude with Mach number Sweep

Appendix B: TIHE Engine Selection Data and Graphs

Engine Type	Engine #	Xover Mach	Xover altitude (ft)	Max Power (MW)	Mach at Max	Altitude at Max (ft)	Tt4 at Max (deg R)	Min Power (MW)	Mach at Min	Alt at Min (ft)	Tt4 at Min (deg R)	Conv Fuel used (lbf)	Cruise Power (MW)
Single Spool Turbojet	tjs4206	0.4	20 k	8.244	0.4	20000	1981.7	3.756	0.6	63250	2702.6	4475	3.756
Dual Spool Turbojet	tj4209	0.4	20 k	8.077	0.4	20000	1967.2	3.867	0.575	55000	2446.7	4380	3.873
Split Stream Turbofan	tfs4213	0.4	20 k	5.916	0.4	20000	2123.9	2.987	0.575	55000	2620.7	3247	3.051
Mixed Stream Turbofan	tfm4213	0.4	20 k	6.244	0.4	20000	2247.3	2.748	0.6	63250	2948.9	3608	2.748
Single Spool Turbojet	tjs4206	0.4	30k	5.228	0.4	30000	1842	3.776	0.567	55000	2372.7	3997	3.795
Dual Spool Turbojet	tj4300	0.4	30k	5.187	0.4	30000	1846.4	3.866	0.567	55000	2448.2	3937	3.916
Split Stream Turbofan	tfs4307	0.4	30k	3.579	0.4	30000	2043.3	2.798	0.567	55000	2668.7	2725	2.896
Mixed Stream Turbofan	tfm4213	0.4	30k	4.035	0.4	30000	2116.9	2.761	0.6	63351	2972.8	3225	2.761
Single Spool Turbojet	tjs4402	0.4	40k	3.916	0.6	60000	2562.9	3.672	0.55	55000	2319.9	3967	3.807
Dual Spool Turbojet	tj4303	0.4	40k	4.033	0.6	60000	2665	3.712	0.4	40000	1853.7	3931	3.935
Split Stream Turbofan	tfs4403	0.4	40k	2.976	0.6	60000	2931.3	2.565	0.4	40000	2056.8	2723	2.924
Mixed Stream Turbofan	tfm4403	0.4	40k	2.888	0.4	40000	2114.9	2.75	0.55	55000	2615	3189	2.775
Mixed Stream Turbofan	tfm5407	0.4	40k	2.65	0.6	60000	2928.2	2.493	0.4	40000	2113	2653	2.567
Single Spool Turbojet	tjs5203	0.5	20 k	13.38	0.5	20000	2295	3.856	0.6	63250	2749.3	5151	3.856
Dual Spool Turbojet	tj5208	0.5	20 k	13.62	0.5	20000	2360.9	3.888	0.6	63250	2813.9	5104	3.888
Split Stream Turbofan	tfs5200	0.5	20 k	9.811	0.5	20000	2509.2	3.057	0.6	63250	3000.3	3787	3.057
Mixed Stream Turbofan	tfm5200	0.5	20 k	9.25	0.5	20000	2659.7	2.588	0.6	63250	3033.3	4008	2.588
Single Spool Turbojet	tjs5303	0.5	30k	8.358	0.5	30000	2115.3	3.757	0.6	63351	2638.7	4320	3.757
Dual Spool Turbojet	tj5308	0.5	30k	8.303	0.5	30000	2147.1	3.898	0.6	63351	2789.1	4252	3.898
Split Stream Turbofan	tfs5303	0.5	30k	6.18	0.5	30000	2327.6	3.093	0.6	63351	3021.3	3184	3.093
Mixed Stream Turbofan	tfm5309	0.5	30k	5.871	0.5	30000	2338.2	2.843	0.6	63351	2937.7	3098	2.843
Single Spool Turbojet	tjs5408	0.5	40k	5.096	0.5	40000	1985.9	3.745	0.6	63465	2609.5	3864	3.745
Dual Spool Turbojet	tj5403	0.5	40k	5.16	0.5	40000	2084.8	3.922	0.6	63465	2823.6	3883	3.922
Split Stream Turbofan	tfs5403	0.5	40k	3.818	0.5	40000	2265.7	3.006	0.575	55000	2662.7	2835	3.023
Mixed Stream Turbofan	tfm5407	0.5	40k	3.42	0.5	40000	2336.7	2.567	0.6	63465	3056.6	2603	2.567
Single Spool Turbojet	tjs6206	0.6	20 k	23.29	0.6	20000	2519.3	3.604	0.6	63250	2374.8	6585	3.604
Dual Spool Turbojet	tj6210	0.6	20 k	23.3	0.6	20000	2609.7	3.774	0.6	63250	2559.4	6525	3.774
Split Stream Turbofan	tfs6203	0.6	20 k	17.82	0.6	20000	3023.4	3.039	0.6	63250	2976.7	4974	3.039
Mixed Stream Turbofan	tfm6211	0.6	20 k	15.31	0.6	20000	3062	2.631	0.6	63250	3011.5	5077	2.631
Single Spool Turbojet	tjs6300	0.6	30k	14.17	0.6	30000	2382.5	3.668	0.6	63351	2470.5	5138	3.668
Dual Spool Turbojet	tj6305	0.6	30k	14.23	0.6	30000	2478.5	3.814	0.6	63351	2650.9	5085	3.814
Split Stream Turbofan	tfs6310	0.6	30k	10.84	0.6	30000	2790.2	3.062	0.6	63351	3001.6	3888	3.062
Mixed Stream Turbofan	tfm6305	0.6	30k	9.418	0.6		2830.9	2.657	0.6	63351	3033.5	3860	2.657
Single Spool Turbojet	tjs6405	0.6	40k	8.423	0.6	40000	2329.5	3.743	0.6	63465	2590.2	4278	3.743
Dual Spool Turbojet	tj6403	0.6	40k	8.453	0.6	40000	2364.1	3.862	0.6	63465	2697.5	4230	3.862
Split Stream Turbofan	tfs6408	0.6	40k	6.316	0.6	40000	2654.9	2.988	0.6	63465	3030.4	3144	2.988
Mixed Stream Turbofan	tfm6401	0.6	40k	5.687	0.6	40000	2694.4	2.675	0.6	63465	3055.3	3914	2.675

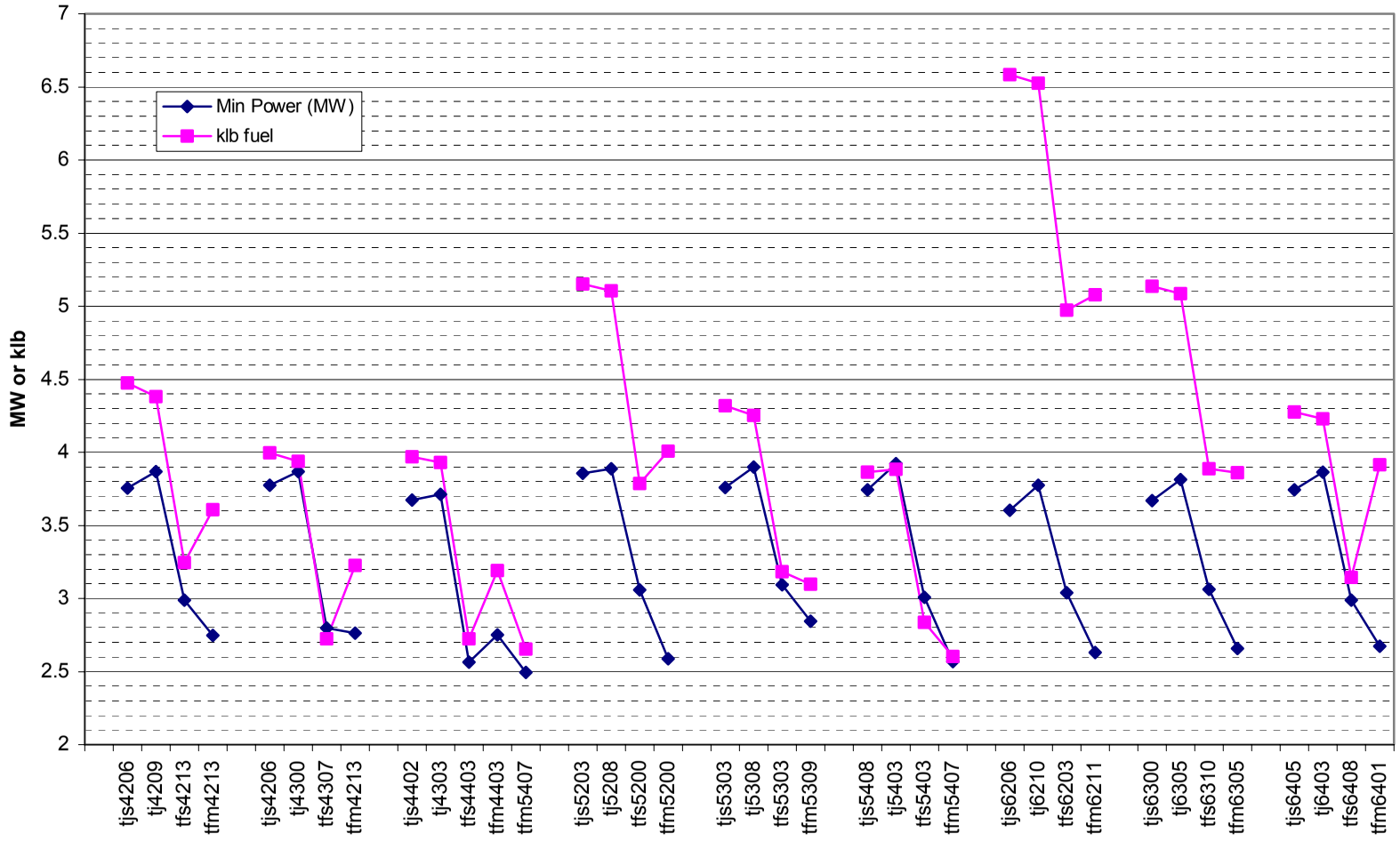

Hybrid engine performance: Conventional fuel consumption (k lbf) and Min power (MW)

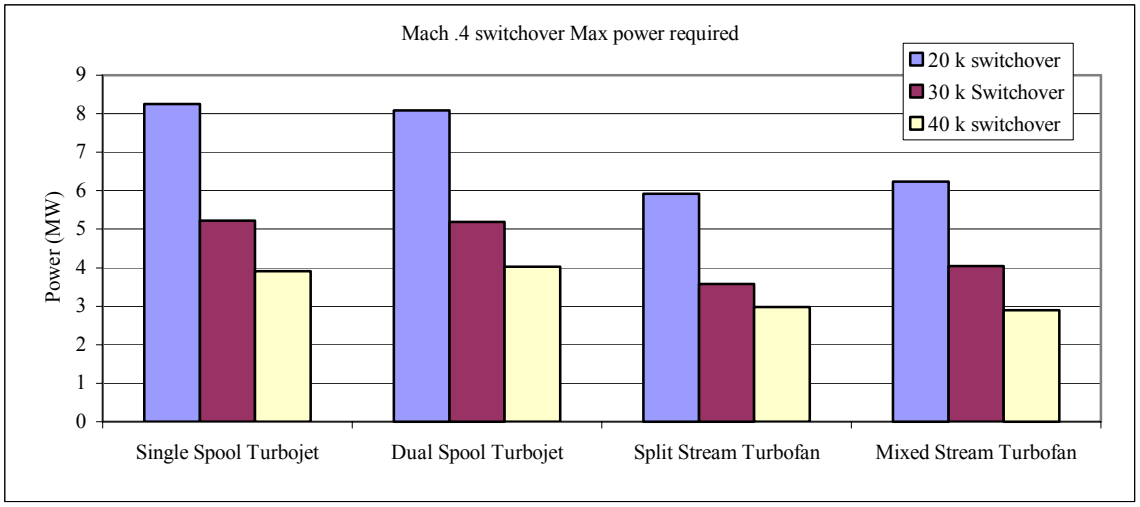

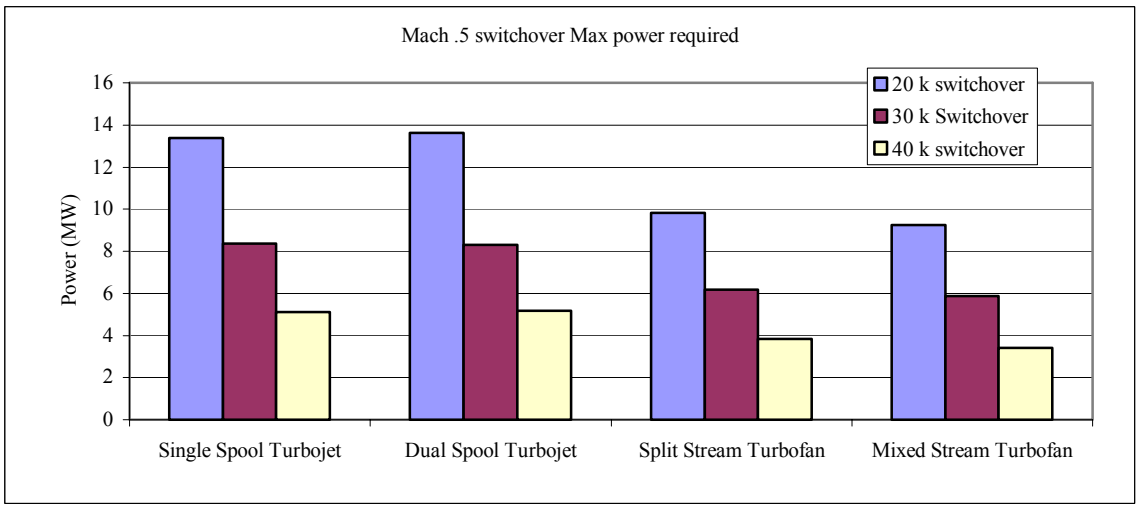

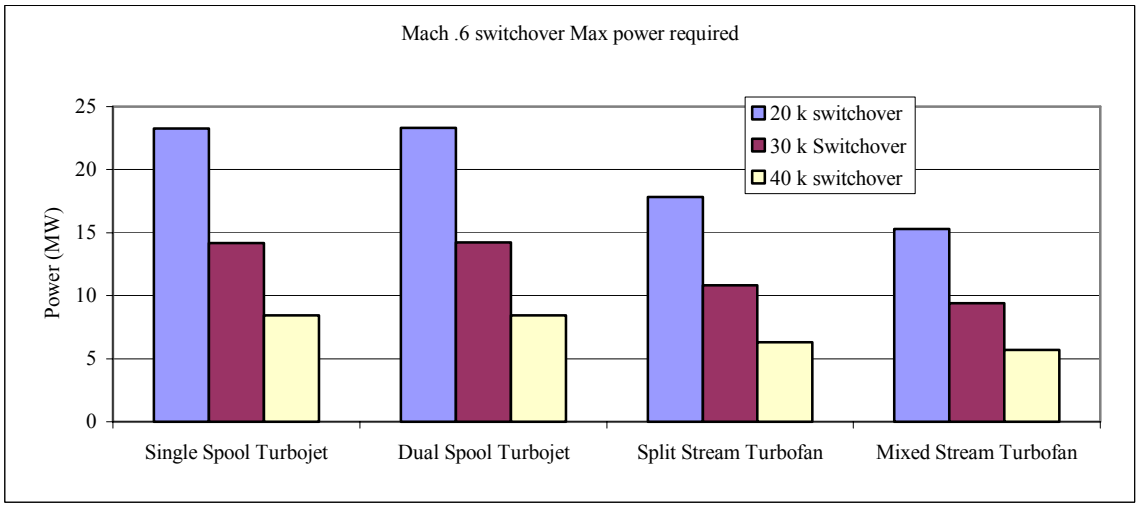

Optimized TIHE Engines: Comparison at specific Mach number with altitude Sweep

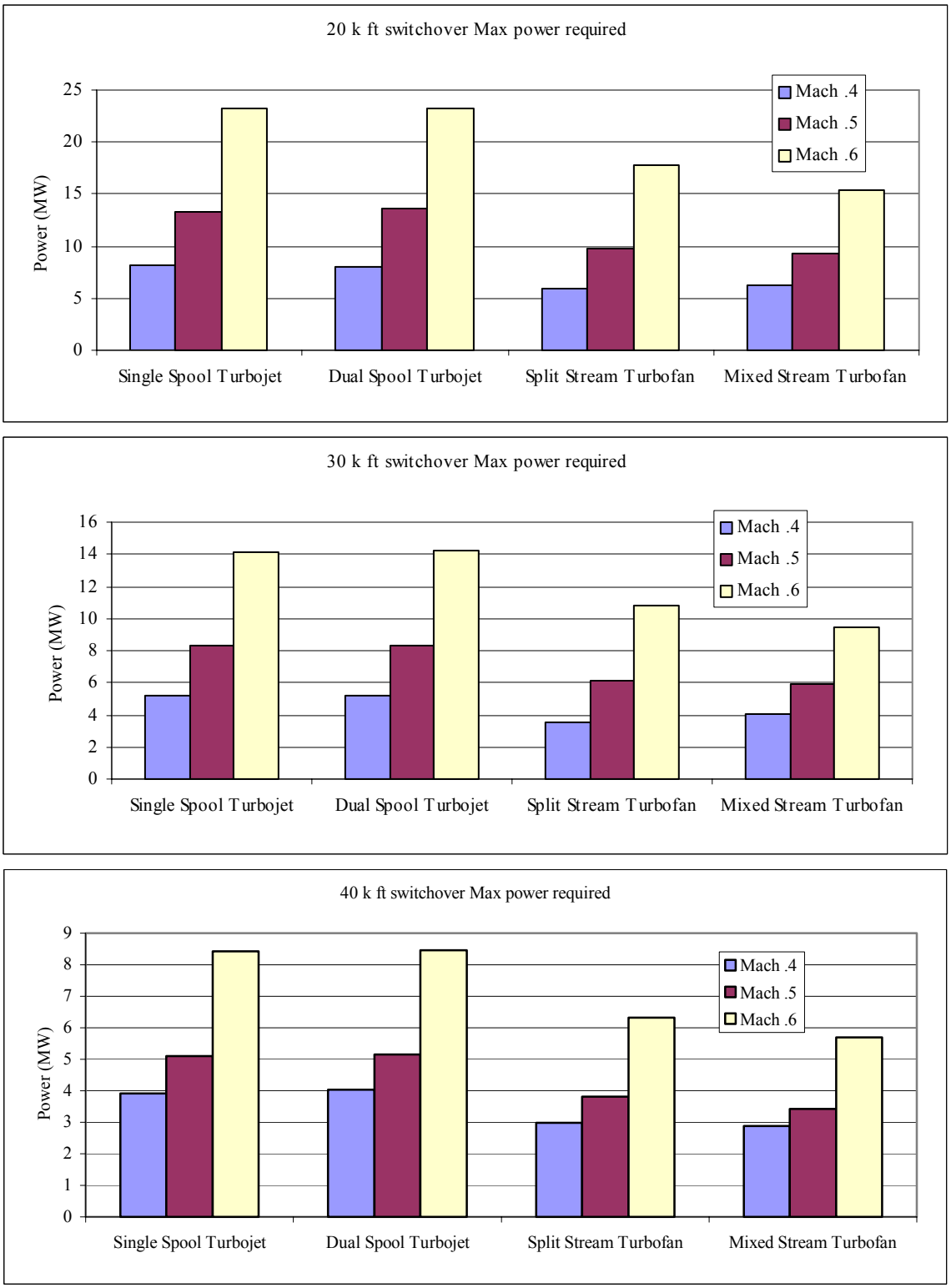

Optimized TIHE Engines: Comparison at specific altitude with Mach number Sweep

Appendix C: Shield Weight Calculations

Test	Power Required (MW)	Hafnium Amount (kg)	% of Radiation	Radiation Output (MW)	Radius (m)	Intensity phi (W/m^2)	Dosage (Rad/sec)	Equipment Tolerance (rad/sec)	Dose Buildup Factor	Relaxation Length	Mass Attenuation Coefficient (cm^2/g)	Shield Thickness (cm)	Shield Load (kg/m^2)	Shield distance (m)	Shield Area (m^2)	Weight of Shield (N)	Weight in LBF (lbf)	Weight of Sphere (lbf)
Baseline	5.00E+06	23.262	5%	2.50E+05	3	2210.49	596.831	1.00E-02	2.413	11.878	0.15	6.946199	791.867	0.5	1.571	12202	2743.32	5486.6362
Shield Distance	5.00E+06	23.262	5%	2.50E+05	3	2210.49	596.831	1.00E-02	2.413	11.878	0.15	6.946199	791.867	1	6.283	48809	10973.3	21946.545
Shield Distance	5.00E+06	23.262	5%	2.50E+05	3	2210.49	596.831	1.00E-02	2.413	11.878	0.15	6.946199	791.867	2	25.13	195236	43893.1	87786.179
% of Radiation Escape	5.00E+06	23.262	10%	5.00E+05	3	4420.97	1193.662	1.00E-02	2.467	12.593	0.15	7.364327	839.533	0.5	1.571	12937	2908.45	5816.906
% of Radiation Escape	5.00E+06	23.262	50%	2.50E+06	3	22104.9	5968.31	1.00E-02	2.593	14.252	0.15	8.334503	950.133	0.5	1.571	14641	3291.61	6583.2244
% of Radiation Escape	5.00E+06	23.262	90%	4.50E+06	3	39788.7	10742.96	1.00E-02	2.639	14.858	0.15	8.688889	990.533	0.5	1.571	15264	3431.57	6863.1453
Equipment Tolerance	5.00E+06	23.262	5%	2.50E+05	3	2210.49	596.831	1.00E-06	2.765	21.224	0.15	12.4117	1414.93	0.5	1.571	21803	4901.85	9803.7015
Equipment Tolerance	5.00E+06	23.262	5%	2.50E+05	3	2210.49	596.831	1.00E-01	2.24	9.494	0.15	5.552047	632.933	0.5	1.571	9753.2	2192.71	4385.4289
Equipment Tolerance	5.00E+06	23.262	5%	2.50E+05	3	2210.49	596.831	1.00E+00	2.03	7.1	0.15	4.152047	473.333	0.5	1.571	7293.8	1639.8	3279.6024
50 MW equipment	5.00E+07	232.62	5%	2.50E+06	3	22104.9	5968.31	1.00E-02	2.587	14.25	0.15	8.333333	950	0.5	1.571	14639	3291.15	6582.3005
50 MW Human	5.00E+07	232.62	5%	2.50E+06	3	22104.9	5968.31	1.00E-06	2.745	23.519	0.15	13.7538	1567.93	0.5	1.571	24161	5431.9	10863.798
Equipment Distance	5.00E+06	23.262	5%	2.50E+05	0.5	79577.5	21485.92	1.00E-02	2.647	15.554	0.15	9.095906	1036.93	0.5	1.571	15979	3592.32	7184.6388
Equipment Distance	5.00E+06	23.262	5%	2.50E+05	1	19894.4	5371.479	1.00E-02	2.581	14.142	0.15	8.270175	942.8	0.5	1.571	14528	3266.21	6532.4136
Equipment Distance	5.00E+06	23.262	5%	2.50E+05	2	4973.59	1342.87	1.00E-02	2.5	12.724	0.15	7.440936	848.267	0.5	1.571	13071	2938.71	5877.417
Equipment Distance	5.00E+06	23.262	5%	2.50E+05	3	2210.49	596.831	1.00E-02	2.413	11.878	0.15	6.946199	791.867	0.5	1.571	12202	2743.32	5486.6362
Equipment Distance	5.00E+06	23.262	5%	2.50E+05	5	795.775	214.8592	1.00E-02	2.368	10.837	0.15	6.337427	722.467	0.5	1.571	11133	2502.89	5005.7818
tfs4403	3.50E+06	16.283	5%	175000	3	1547.34	417.7817	1.00E-02	2.419	11.523	0.15	6.738596	768.2	0.5	1.571	11838	2661.33	5322.6561
mod tfs4403	3.10E+06	14.422	5%	155000	3	1370.5	370.0352	1.00E-02	2.41	11.399	0.15	6.666082	759.933	0.5	1.571	11710	2632.69	5265.3785
tfm5407	3.06E+06	14.222	5%	152850	3	1351.49	364.9025	1.00E-02	2.409	11.384	0.15	6.65731	758.933	0.5	1.571	11695	2629.22	5258.4498
TIHEX1	2.90E+06	14.222	5%	144800	3	1280.31	345.6845	1.00E-02	2.405	11.328	0.15	6.624561	755.2	0.5	1.571	11637	2616.29	5232.5825
TIHEX2	2.45E+06	11.398	5%	122500	3	1083.14	292.4472	1.00E-02	2.392	11.156	0.15	6.523977	743.733	0.5	1.571	11461	2576.57	5153.133

Appendix D: Final TIHEX AEDsys Values and Calculations

Table D-1: TIHEX 1 Hybrid engine AEDsys summary pages and Heat power calculations

leg	name	Mach	altitude	AO	A9	T(lbf)	TSFC(1/hr)	Phi I+N	Limit	TT4 (deg R)	hpr (BTU/lb)	Burner Efficiency	fuel consumption (lb/hr)	actual energy(BTU/hr)	actual energy(Watts)
TIHEX 1															
1	Warm u	0	0	3.649	3.015	5241	0.6463	0.16098	Tt4 Max	3200	18000	0.98	3387.2583	5.975E+07	1.750E+07
2	1-2 B	0	0	3.646	3.013	5211	0.651078	0.10057	Tt4 Max	3200	18000	0.98	3392.7675	5.985E+07	1.753E+07
3	1-2 C	0.1958	0	3.634	3.011	5081	0.671932	0.03868	Tt4 Max	3200	18000	0.98	3414.0865	6.022E+07	1.764E+07
4	2-3 Ea	0.2906	0	4.991	3.176	5049	0.586465	0.01214	PIC Max	3034.9	18000	0.98	2961.0618	5.223E+07	1.530E+07
5	Xover-	0.4	40000	3.388	2.98	739	0.708471	0.01058	Thrust=Drag	2228.5	18000	0.98	523.56007	9.236E+06	2.705E+06
6	Xover-	0.4	40000	3.383	2.98	735	0.70928	0.01078	Thrust=Drag	2225.9	18000	0.98	521.3208	9.196E+06	2.693E+06
7	Xover-	0.4	40000	3.379	2.98	732	0.7101	0.01098	Thrust=Drag	2223.3	18000	0.98	519.7932	9.169E+06	2.685E+06
8	Xover-	0.4	40000	3.373	2.98	729	0.711208	0.01124	Thrust=Drag	2220.1	18000	0.98	518.47063	9.146E+06	2.679E+06
9	40k TI	0.4	40000	3.368	2.98	725	0.712036	0.01145	Thrust=Drag	2217.5	18000	0.98	516.2261	9.106E+06	2.667E+06
10	45k TI	0.45	45000	3.612	2.975	714	0.721868	0.0151	Thrust=Drag	2398.3	18000	0.98	515.41375	9.092E+06	2.663E+06
11	50k TI	0.5	50000	3.858	2.993	703	0.735035	0.01722	Thrust=Drag	2590	18000	0.98	516.72961	9.115E+06	2.670E+06
12	55k TI	0.55	55000	4.14	3.062	690	0.74922	0.01682	Thrust=Drag	2792.2	18000	0.98	516.9618	9.119E+06	2.671E+06
13	60k TI	0.6	60000	4.623	3.227	743	0.754226	0.00899	Thrust=Drag	3078.6	18000	0.98	560.38992	9.885E+06	2.895E+06
14	TIHE C	0.6	58822	4.521	3.196	741	0.756585	0.01222	PIC Max	3024.8	18000	0.98	560.62949	9.890E+06	2.896E+06
15	xover2	0.4	40000	3.368	2.98	725	0.712036	0.01145	Thrust=Drag	2217.5	18000	0.98	516.2261	9.106E+06	2.667E+06
16	xover2	0.4	40000	3.364	2.98	722	0.712862	0.01166	Thrust=Drag	2215	18000	0.98	514.68636	9.079E+06	2.659E+06
17	xover2	0.4	40000	3.359	2.98	719	0.713685	0.01186	Thrust=Drag	2212.5	18000	0.98	513.13952	9.052E+06	2.651E+06
18	xover2	0.4	40000	3.355	2.981	716	0.714513	0.01207	Thrust=Drag	2210.1	18000	0.98	511.59131	9.024E+06	2.643E+06
19	Sea Le	0.1765	0	1.805	3.191	756	1.074817	0.00138	Thrust=Drag	1773.9	18000	0.98	812.56165	1.433E+07	4.198E+06

Table D-2: TIHEX 2 Hybrid engine AEDsys summary pages and Heat power calculations

TIHEX2

leg	*name*	*Mach*	*altitude*	*AO*	*A9*	*T(lbf)*	*TSFC(1/hr)*	*Phi I+N*	*Limit*	*TT4 (deg R)*	*hpr (BTU/lb)*	*Burner Efficiency*	*fuel consumption (lb/hr)*	*actual energy(BTU/hr)*	*actual energy(Watts)*
1	Warm u	0	0	3.649	3.015	5241	0.6463	0.16098	Tt4 Max	3200	18000	0.98	3387.2583	5.975E+07	1.750E+07
2	1-2 B	0	0	3.646	3.013	5211	0.651078	0.10057	Tt4 Max	3200	18000	0.98	3392.7675	5.985E+07	1.753E+07
3	1-2 C	0.1757	0	3.637	3.012	5113	0.666662	0.04855	Tt4 Max	3200	18000	0.98	3408.6428	6.013E+07	1.761E+07
4	2-3 Ea	0.2906	0	4.991	3.176	5049	0.586465	0.01214	PIC Max	3034.9	18000	0.98	2961.0618	5.223E+07	1.530E+07
5	Xover-	0.4	40000	3.216	2.984	618	0.74519	0.02021	Thrust=Drag	2133.1	18000	0.98	460.52742	8.124E+06	2.379E+06
6	Xover-	0.4	40000	3.213	2.984	616	0.745963	0.02042	Thrust=Drag	2131.4	18000	0.98	459.51321	8.106E+06	2.374E+06
7	Xover-	0.4	40000	3.21	2.984	614	0.746729	0.02063	Thrust=Drag	2129.8	18000	0.98	458.49161	8.088E+06	2.369E+06
8	Xover-	0.4	40000	3.207	2.984	612	0.747497	0.02084	Thrust=Drag	2128.1	18000	0.98	457.46816	8.070E+06	2.363E+06
9	40k TI	0.4	40000	3.204	2.984	610	0.748255	0.02105	Thrust=Drag	2126.5	18000	0.98	456.43555	8.052E+06	2.358E+06
10	45k TI	0.45	45000	3.444	2.977	604	0.753025	0.02551	Thrust=Drag	2300.1	18000	0.98	454.8271	8.023E+06	2.350E+06
11	50k TI	0.5	50000	3.665	2.977	592	0.763621	0.02916	Thrust=Drag	2481.2	18000	0.98	452.06363	7.974E+06	2.336E+06
12	55k TI	0.55	55000	3.899	3.015	576	0.777124	0.03054	Thrust=Drag	2668.1	18000	0.98	447.62342	7.896E+06	2.313E+06
13	60k TI	0.6	60000	4.29	3.132	610	0.777573	0.02177	Thrust=Drag	2925.7	18000	0.98	474.31953	8.367E+06	2.450E+06
14	TIHE C	0.6	63354	4.503	3.196	597	0.771798	0.01271	PIC Max	3050.2	18000	0.98	460.76341	8.128E+06	2.380E+06
15	xover2	0.4	40000	3.204	2.984	610	0.748255	0.02105	Thrust=Drag	2126.5	18000	0.98	456.43555	8.052E+06	2.358E+06
16	xover2	0.4	40000	3.201	2.984	608	0.749014	0.02126	Thrust=Drag	2125	18000	0.98	455.40051	8.033E+06	2.353E+06
17	xover2	0.4	40000	3.198	2.984	606	0.749768	0.02147	Thrust=Drag	2123.4	18000	0.98	454.35941	8.015E+06	2.347E+06
18	xover2	0.4	40000	3.196	2.984	604	0.750519	0.02167	Thrust=Drag	2121.8	18000	0.98	453.31348	7.996E+06	2.342E+06
19	Sea Le	0.2	0	1.833	3.178	719	1.139939	0.01193	Thrust=Drag	1778.7	18000	0.98	819.61614	1.446E+07	4.234E+06
20	Sea Le	0.2	0	1.831	3.179	716	1.143306	0.0123	Thrust=Drag	1777.3	18000	0.98	818.6071	1.444E+07	4.229E+06
21	Sea Le	0.2	0	1.828	3.18	712	1.146611	0.01253	Thrust=Drag	1775.9	18000	0.98	816.38703	1.440E+07	4.218E+06

Table D-1: TIHEX 1 & 2 Hybrid engines AEDsys summary pages and Flight Performance calculations

Leg	Title	PI	Beta initial	Beta Final	Wt Change (lbf)	Drag (lbf)	Thrust (Lbf)	Time (sec)	Distance (nmi)	Fuel Consumed Totals (lbf)
TIHEX 1										
1	Warm u	0.99779	1	0.99779	56	0	5241	60	0	56
2	1-2 B	0.99704	0.99779	0.99484	76	2967	5211	59.9	1.12	132
3	1-2 C	0.99989	0.99484	0.99473	3	2967	5081	3	0.11	135
4	2-3 Ea	0.96927	0.99473	0.96416	783	752	5049	1091.2	56.94	918
5	Xover-	0.99539	0.96416	0.95971	114	739	739	784.6	50	1032
6	Xover-	0.99538	0.95971	0.95528	113	735	735	784.6	50	1145
7	Xover-	0.99538	0.95528	0.95087	113	732	732	784.6	50	1258
8	Xover-	0.99537	0.95087	0.94647	113	729	729	784.6	50	1371
9	40k TI	1	0.94647	0.94647	0	725	725	0	0	1371
10	45k TI	1	0.94647	0.94647	0	714	714	0	0	1371
11	50k TI	1	0.94647	0.94647	0	703	703	0	0	1371
12	55k TI	1	0.94647	0.94647	0	690	690	0	0	1371
13	60k TI	1	0.94647	0.94647	0	743	743	0	0	1371
14	TIHE C	1	0.94647	0.94647	0	741	741	0	0	1371
15	xover2	0.99537	0.94647	0.94208	112	725	725	784.6	50	1483
16	xover2	0.99536	0.94208	0.93771	112	722	722	784.6	50	1595
17	xover2	0.99535	0.93771	0.93335	112	719	719	784.6	50	1707
18	xover2	0.99535	0.93335	0.92901	111	716	716	784.6	50	1818
19	Sea Le	0.9664	0.92901	0.8978	799	756	756	3600	0	2617
TIHEX 2										
1	Warm u	0.99726	0.806	0.80379	56	0	5241	60	0	56
2	1-2 B	0.99788	0.80379	0.80209	44	2393	5211	37.7	0.63	100
3	1-2 C	0.99986	0.80209	0.80198	3	2393	5113	3	0.1	103
4	2-3 Ea	0.97009	0.80198	0.77799	614	652	5049	852.4	44.39	717
5	Xover-	0.99498	0.77799	0.77408	100	618	618	784.6	50	817
6	Xover-	0.99496	0.77408	0.77019	100	616	616	784.6	50	917
7	Xover-	0.99495	0.77019	0.76629	100	614	614	784.6	50	1017
8	Xover-	0.99493	0.76629	0.76241	99	612	612	784.6	50	1116
9	40k TI	1	0.76241	0.76241	0	610	610	0	0	1116
10	45k TI	1	0.76241	0.76241	0	604	604	0	0	1116
11	50k TI	1	0.76241	0.76241	0	592	592	0	0	1116
12	55k TI	1	0.76241	0.76241	0	576	576	0	0	1116
13	60k TI	1	0.76241	0.76241	0	610	610	0	0	1116
14	TIHE C	1	0.76241	0.76241	0	597	597	0	0	1116
15	xover2	0.99492	0.76241	0.75854	99	610	610	784.6	50	1215
16	xover2	0.99491	0.75854	0.75468	99	608	608	784.6	50	1314
17	xover2	0.99489	0.75468	0.75082	99	606	606	784.6	50	1413
18	xover2	0.99488	0.75082	0.74697	98	604	604	784.6	50	1511
19	Sea Le	0.98392	0.74697	0.73497	307	719	719	1360.6	50	1818
20	Sea Le	0.9837	0.73497	0.72298	307	716	716	1360.6	50	2125
21	Sea Le	0.98675	0.72298	0.7134	245	712	712	1088.5	40	2370

VITA

Captain Christopher E. Hamilton was born in Honolulu, Hawaii. He graduated from Punahou School in 1990 and entered undergraduate studies at the University of Michigan in Ann Arbor, Michigan. He graduated with a Bachelor of Science degree in Aerospace Engineering in April 1995. He received his commission on 28 April 1995 and entered active duty in the USAF in July 1995.

His first assignment was an eight-month training program, including Undergraduate Space and Missile Training and Initial Qualifying Training in the Minuteman III ICBM Weapon System, at Vandenberg AFB, California. In February 1996, he was assigned to the 564th Missile Squadron at Malmstrom AFB, Montana as a Missile Combat Crew Member. Chris held several positions in ICBM operations and training at Malmstrom AFB, culminating in his selection as Senior Operations Instructor for the 341st Space Wing.

In August 2000, he entered the Aeronautical Engineering graduate program at the School of Engineering and Management, Air Force Institute of Technology. Upon completion of his Master of Science degree, he will be assigned as an aeronautical research engineer to the Propulsion Directorate of the Air Force Research Laboratory located at Wright-Patterson AFB, Ohio.

REPORT DOCUMENTATION PAGE

Form Approved
OMB No. 074-0188

1. REPORT DATE *(DD-MM-YYYY)*	2. REPORT TYPE	3. DATES COVERED *(From – To)*
26-03-2002	Master's Thesis	Jun 2001 – Mar 2002

4. TITLE AND SUBTITLE
DESIGN STUDY OF TRIGGERED ISOMER HEAT EXCHANGER-COMBUSTION HYBRID JET ENGINE FOR HIGH ALTITUDE FLIGHT

5a. CONTRACT NUMBER

5b. GRANT NUMBER

5c. PROGRAM ELEMENT NUMBER

6. AUTHOR(S)
Hamilton, Christopher E., Captain, USAF

5d. PROJECT NUMBER

5e. TASK NUMBER

5f. WORK UNIT NUMBER

7. PERFORMING ORGANIZATION NAMES(S) AND ADDRESS(S)
Air Force Institute of Technology
Graduate School of Engineering and Management (AFIT/ENY)
2950 P Street, Building 640
WPAFB OH 45433-7765

8. PERFORMING ORGANIZATION REPORT NUMBER
AFIT/GAE/ENY/02-6

9. SPONSORING/MONITORING AGENCY NAME(S) AND ADDRESS(ES)

10. SPONSOR/MONITOR'S ACRONYM(S)

11. SPONSOR/MONITOR'S REPORT NUMBER(S)

12. DISTRIBUTION/AVAILABILITY STATEMENT
APPROVED FOR PUBLIC RELEASE; DISTRIBUTION UNLIMITED.

13. SUPPLEMENTARY NOTES
.

14. ABSTRACT
This study investigated the possibility of utilizing a Triggered Isomer Heat Exchanger (TIHE) within a conventional jet engine in order to increase the endurance of a High Altitude Long Endurance (HALE) Intelligence, Surveillance, and Reconnaissance (ISR) aircraft. Optimizations of the conventional and TIHE engines along with selection of a switchover flight condition, where the aircraft switches from combustion to TIHE operations, were made utilizing engine design and mission analysis software. Radiation shield weights were determined utilizing point source gamma ray shielding methods. The jet engine best suited for the hybrid use, where both combustion and TIHE components located in a single engine, was a mixed stream turbofan engine flying both the conventional and TIHE legs of the mission, with a switchover Mach of 0.4 and switchover altitude of 40,000 ft. With the single hybrid engine, including shield weights and modifications, endurance could easily be extended into weeks instead of days, while also resulting in a 20% drop in takeoff weight of current vehicles. The reduction in weight was due mainly to lower fuel requirements.

15. SUBJECT TERMS
Triggered Isomer, High Altitude Long Endurance, Intelligence, Surveillance, Reconnaissance, Aircraft Propulsion, Turbofan

16. SECURITY CLASSIFICATION OF:			17. LIMITATION OF ABSTRACT	18. NUMBER OF PAGES	19a. NAME OF RESPONSIBLE PERSON
a. REPORT	b. ABSTRACT	c. THIS PAGE			Paul I. King, AFIT/ENY
U	U	U	UU	111	19b. TELEPHONE NUMBER *(Include area code)* (937) 255-3636 x4628

Standard Form 298 (Rev. 8-98)
Prescribed by ANSI Std. Z39-18

Form Approved
OMB No. 074-0188